GeroScience
https://doi.org/10.1007/s11357-024-01133-z

ORIGINAL ARTICLE

Modulation of neural gene networks by estradiol in old rhesus macaque females

Rita Cervera-Juanes · Kip D. Zimmerman · Larry Wilhelm · Dongqin Zhu · Jessica Bodie · Steven G. Kohama · Henryk F. Urbanski

Received: 8 January 2024 / Accepted: 12 March 2024

Abstract The postmenopausal decrease in circulating estradiol (E2) levels has been shown to contribute to several adverse physiological and psychiatric effects. To elucidate the molecular effects of E2 on the brain, we examined differential gene expression and DNA methylation (DNAm) patterns in the nonhuman primate brain following ovariectomy (Ov) and subsequent subcutaneous bioidentical E2 chronic treatment. We identified several dysregulated molecular networks, including MAPK signaling and dopaminergic synapse response, that are associated with ovariectomy and shared across two different brain areas, the occipital cortex (OC) and prefrontal cortex (PFC). The finding that hypomethylation ($p = 1.6 \times 10^{-51}$) and upregulation ($p = 3.8 \times 10^{-3}$) of *UBE2M* across both brain regions provide strong evidence for molecular differences in the brain induced by E2 depletion. Additionally, differential expression ($p = 1.9 \times 10^{-4}$; interaction $p = 3.5 \times 10^{-2}$) of *LTBR* in the PFC provides further support for the role E2 plays in the brain, by demonstrating that the regulation of some genes that are altered by ovariectomy may also be modulated by Ov followed by hormone replacement therapy (HRT). These results present real opportunities to understand the specific biological mechanisms that are altered with depleted E2. Given E2's potential role in cognitive decline and neuroinflammation, our findings could lead to the discovery of novel therapeutics to slow cognitive decline.

Rita Cervera-Juanes and Kip D. Zimmerman contributed equally to this work.

Supplementary Information The online version contains supplementary material available at https://doi.org/10.1007/s11357-024-01133-z.

R. Cervera-Juanes (✉) · L. Wilhelm · D. Zhu · J. Bodie
Department of Translational Neuroscience, Wake Forest University School of Medicine, 1 Medical Center Boulevard, Winston-Salem, NC 27157, USA
e-mail: rcervera@wakehealth.edu

R. Cervera-Juanes · K. D. Zimmerman
Center for Precision Medicine, Wake Forest University School of Medicine, 1 Medical Center Boulevard, Winston-Salem, NC 27157, USA

K. D. Zimmerman
Department of Internal Medicine, Wake Forest University School of Medicine, 1 Medical Center Boulevard, Winston-Salem, NC 27157, USA

S. G. Kohama · H. F. Urbanski
Division of Neuroscience, Oregon National Primate Research Center, Beaverton, OR 97006, USA

H. F. Urbanski
Division of Reproductive & Developmental Sciences, Oregon National Primate Research Center, Beaverton, OR 97006, USA

H. F. Urbanski
Department of Behavioral Neuroscience, Oregon Health & Science University, Portland, OR 97239, USA

Published online: 20 March 2024

Together, this work represents a major step toward understanding molecular changes in the brain that are caused by ovariectomy and how E2 treatment may revert or protect against the negative neuro-related consequences caused by a depletion in estrogen as women approach menopause.

Keywords Aging · DNA methylation · Estradiol · Occipital cortex · Prefrontal cortex · RNA-Seq

Introduction

Estradiol (E2) is mainly produced by the ovaries and is the most physiologically relevant estrogen (others include estrone and estriol). E2 exerts control over numerous biological functions by binding to the intracellular estrogen receptors alpha and beta (ERα and ERβ) [1–5] and the G-protein-coupled receptor GPR30/GPER1 [6].

E2 levels fluctuate throughout the female menstrual cycle, and as women age and go through natural menopause, E2 levels progressively decline. As a reflection of the broad roles of E2, adverse physiological and psychiatric effects accompany the natural decline of E2 levels. These include vasomotor symptoms (hot flashes, night sweats) [7, 8], sleep disturbances [9], somatic symptoms (pains, aches) [7], cognitive performance decline [10], anxiety [7], and depression [7]. Such effects are expected given the E2's neural role in mediating synaptic plasticity [11–16], increasing dendritic spine density, long-term potentiation (LTP) [17], neuroprotective effects [18], and improving cognitive performance [19, 20].

A lack of E2 right after menopause negatively affects learning and memory and increases the risk of neurodegenerative diseases, such as Alzheimer's disease (AD) [21, 22]. The incidence of AD and related dementias is two to three times higher in women than in men, and premature menopause increases this risk [23, 24]. Although surrounded by a lot of debate [25, 26], there is much evidence to suggest that E2 replacement therapy, administered immediately at menopause [27–35], may improve cognitive performance and reduce risk for onset and development of AD [3–5, 24]. These effects highlight E2's role in preserving cognitive function and overall well-being.

Although it does not exactly replicate the natural decline in E2 as seen in healthy women, ovariectomy (Ov) and ovohysterectomy (OvH) have been widely used in preclinical models to investigate the physiological and neural adaptations that take place when the ovarian E2 supply is removed [18]. It should be noted that, although there is neuronal production of E2 with important neuromodulator and neuroprotective functions [36, 37], its sources are androgens, which are mostly produced by the ovaries [38]. Ov and Ov with hormone replacement therapy (Ov-HRT) are implemented as effective cancer treatments and are commonly used for benign gynecologic conditions in women 40 years and older [39]. Furthermore, women who underwent Ov showed a higher risk for the development of dementia, but not if they received Ov-HRT treatment at the time of surgery [33]. Thus, preclinical surgical menopause animal systems become excellent models in which to examine the negative impact of reduced E2 concentrations on molecular and physiological processes, as well as the potential benefits of hormonal replacement therapy (HRT), in women who have experienced abrupt E2 removal.

Among the current preclinical models, nonhuman primates (NHPs) are highly valuable for this research because of their very similar physiology to humans and because females undergo a typical menopausal transition, at around 25 years of age [40]. Our own studies, and others, demonstrated that immediate Ov-HRT in aged surgically menopausal rhesus macaque females showed positive effects on memory [30, 41] and favorable effects on cognition in aged females under an obesogenic diet [42]. Using brain samples from the same females, we identified differential gene expression in the occipital (OC), prefrontal cortex (PFC), hippocampus (HIP), and amygdala (AMG), with enrichment in neuroinflammation in OC and HIP, but inhibition in the AMG with Ov-HRT. Synaptogenesis, circadian rhythm, mitochondrial dysfunction, mTOR, glutamate, serotonin, GABA, dopamine, epinephrine/norepinephrine, glucocorticoid receptor signaling, neuronal NOS, and amyloid processing were exclusively enriched in AMG. As compared to the control group, most of these signaling pathways are downregulated after Ov-HRT, suggesting a protective effect of E2 in Ov-HRT females under a Western-style diet. A follow-up study, using the contralateral AMG from these same females, as well as from a separate cohort of females under a regular chow diet, showed that Ov-HRT (immediate treatment) had lower histological amyloid β plaque density as

compared to placebo females [43]. Furthermore, our own studies showed that E2 treatment clearly improved cognitive performance in the same animals included in the current study [30]. Here, we sought to elucidate the molecular pathways in two cognitive-relevant cortical regions that could be altering brain function and ultimately contributing to such cognitive benefits.

It is well-known that E2 binds to ERα and ERβ, and through the canonical mechanism of action, the E2–ER complex binds to estrogen-responsive elements (ERE) at promoters of target genes regulating their expression. In addition, E2, through binding to EREs, regulates gene expression through neuroepigenetic regulation [44]. After binding to ERE, the ligand-bound ERs recruit chromatin remodelers, such are BAF60 or recruiting CREB-binding protein (CBP), that regulate DNA and histone modifications [45–49]. Intrahippocampal E2 increases DNMT3a and 3b levels and activity, decreases HDAC2 expression, and increases H3 and H4 acetylation, altering memory in ovariectomized mice. Furthermore, DNMT inhibition by 5-AZA inhibited recognition memory [50, 51]. These prior findings support the critical role of DNA methylation (DNAm) in mediating the effects of E2 in brain function.

In the present study, we characterize the transcriptomic and methylomic profile of the brain between elderly ovary intact (OI), Ov females without HRT under a regular chow diet to determine the molecular signatures associated with an abrupt depletion of E2 at a peri-menopausal age. We next evaluate if HRT instituted shortly after Ov can revert any of these changes to maintain an age-matched molecular profile. We focus on two cortical brain regions associated with cognitive function and known to be impacted in aging and dementias. The OC is involved in visuospatial processing, distance and depth perception, color determination, object and face recognition, and memory formation [52, 53]. Damage in this area is linked to hallucinations in dementia patients [54]. The PFC is a central brain structure involved in working memory, temporal processing, decision-making, flexibility, and goal-oriented behavior [55]. In the context of AD, neurodegeneration and neural damage have been reported in the PFC and OC, in the latter case with an association to early onset [56, 57].

The present study focused on elucidating the molecular effects of E2 on the primate brain by examining the differential gene expression and DNAm patterns in OI and following Ov and subsequent E2 treatment. With this model, we have identified a number of dysregulated molecular networks that are associated with Ov and are shared across two different regions of the brain, OC and PFC. The latter is particularly susceptible to age-associated neuropathologies such as AD and frontotemporal lobar degeneration (FTLD). Our results suggest extensive molecular differences in the brain induced by E2 depletion. We have also identified a number of Ov-related molecular differences that appear to be modulated by Ov-HRT treatment. These changes offer valuable insights into the neurobiological consequences of E2 deficiency and potential alternative therapeutics that could be more targeted.

Methods

Subjects

This study was approved by the Oregon National Primate Research Center (ONPRC) Institutional Animal Care and Use Committee and used 18 old (range = 15.4–19.2 years, at the beginning of the study) female rhesus macaques (*Macaca mulatta*). The median lifespan of this species in captivity is ~ 25 years [58, 59], and in the range of pre- to peri-menopausal endocrine status [40, 60]. The animals were socially housed indoors in paired cages under controlled environmental conditions—24 °C temperature, 12-h light and 12-h darkness photoperiods (lights on at 07:00 h) and were cared for by the ONPRC Division of Comparative Medicine in accordance with the National Research Council's Guide for the Care and Use of Laboratory Animals. All females were fed a specially prepared balanced and semipurified diet low in phytoestrogens, as described [30]. The diet was prepared in the ONPRC's kitchen bimonthly and kept frozen until use. Daily meals at ~ 08:00 h and ~ 15:00 h were supplemented with fresh fruits or vegetables; fresh drinking water was available ad libitum. Additional enrichment included watching video programs and interactions with the Behavioral Science Unit staff and animal care technicians.

Ovariectomy and estradiol supplementation

Before Ov, all of the females were showing menstrual cycles and were therefore considered to be premenopausal at the beginning of the study. Except for the ovary intact (OI, $n=4$) females, the rest of the animals were Ov, resulting in E2 levels below 20 pg/mL. Half of the females ($n=6$, Ov-HRT) were started on HRT ~ 2.5 months post-Ov in the form of subcutaneous E2-containing elastomer capsules, which achieved serum E2 concentrations of 94.3 ± 20.5 pg/mL; the other half ($n=8$) received empty capsules (placebo), which achieved serum E2 concentrations of < 30 pg/mL on average across ~ 48 months (age at end of study, 19.4–23.2 years). Serum E2 was measured every 2 months and the capsule was replaced or its size adjusted as deemed appropriate [30].

Euthanasia

After the ~ 4-year duration of the study, a detailed necropsy protocol previously used in our laboratory was used to systematically collect brain tissues from all subjects; other body tissues were made available to other investigators for unrelated postmortem studies. OI females were at the follicular phase at necropsy (based on menstrual cycle records and terminal serum estradiol and progesterone concentrations). Briefly, monkeys were sedated with ketamine (10 mg/kg) and administered with pentobarbital, followed by exsanguination, as recommended by the 2013 Edition of the American Veterinary Medical Association Guidelines for the Euthanasia of Animals. Brains were quickly removed, and the right hemisphere was dissected to isolate the different brain regions. Briefly, the dorsal and ventral banks of the PFC were collected around the primary sulcus. The OC was removed from the caudal tip of the occipital lobe. All tissues were wrapped in aluminum foil, immediately frozen in liquid nitrogen, and then archived at − 80 °C. See Fig. 1 for the experimental design.

DNA/RNA isolation

Genomic DNA and RNA were extracted from each brain region using the All-Prep DNA/RNA/miRNA Universal kit (Qiagen Sciences Inc., Germantown, MD) following the manufacturer's recommendations. Briefly, each brain region was pulverized, and ~ 30 mg of tissue was used for DNA/RNA isolation.

cDNA library construction

For stranded RNA-seq, cDNA libraries were prepared with the TruSeq stranded mRNA library prep Kit (cat# RS-122–2101, Illumina, San Diego, CA, USA). The resulting libraries were sequenced on a HiSeq 4000 (Genomics & Cell Characterization Core Facility, University of Oregon) using a paired-end run (2×150 bases). A minimum of 100 M reads was generated from each library.

RNA-Seq processing and calling

Raw sequences were examined for quality using FastQC [61]. Phred scores (probability a base was called correctly) and GC content were observed for abnormalities. After initial quality control of the reads was completed, alignment was performed using

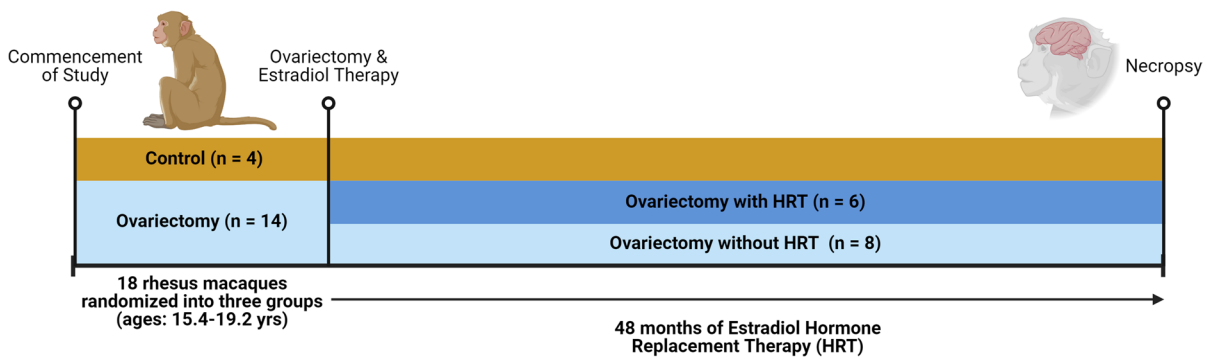

Fig. 1 Experimental design

STAR two-pass alignment [62]. Reads were aligned to the *Macaca mulatta* assembly (Mmul_10) and scored on how well they corresponded to the reference genome and whether or not they map to multiple positions across the genome. Low-scoring reads, usually short and poor-quality reads, were not retained (mapping quality score < 2). Post-alignment, reads were quantified at the gene level using the program featureCounts [63], and DESeq2 [64] was used to transform gene counts and estimate fold-change values for differentially expressed genes. Genes that had either an average read count below 5, missing values for more than one-third of the samples, or a coefficient of variation greater than 50 in the control samples were dropped to remove noisy and lowly expressed genes.

Differential expression analysis

Differential expression analysis was computed in DESeq2 where the gene expression values were evaluated as the outcome in a negative binomial generalized linear model [64]. Whether or not the animal had undergone Ov was the predictor of the primary model we computed. This analysis was computed only in animals that had not received Ov-HRT treatment. Given no significant differences in age between animals and all of them are all much older females (~ 25 years) in the same stage of life and the limited power of the study, we did not adjust for age as a covariate. A Benjamini–Hochberg false discovery rate (FDR) was applied to the unadjusted *p*-value to account for multiple comparisons [65]. We repeated this same analysis in animals treated with Ov-HRT. In addition to these models, to find differences directly related to Ov, we tested the interaction between Ov-HRT and Ov. To enable this analysis, we replicated the control samples (OI) into two groups, one labeled as having received Ov-HRT treatment, and the other as having not received HRT treatment. We recognize that comparing both Ov groups to the same exact set of controls (OI) will lead to false positives, but we primarily used the test of interaction as a way of rapidly identifying genes associated with Ov that are potentially modified by Ov-HRT treatment. As expected, Benjamin–Hochberg FDR adjustment left no interaction results, so we considered interaction results that met an unadjusted $p < 0.05$, particularly because computing the interaction globally for all genes was not our main interest. We were primarily interested in genes that showed expression changes related to Ov that no longer showed association with Ov with Ov-HRT treatment. To obtain a general set of genes that fit this criterion, we filtered the results to include only genes that showed suggestive evidence of Ov association (unadjusted $p < 0.05$) without Ov-HRT treatment and little evidence of Ov association with Ov-HRT treatment (unadjusted $p > 0.1$). From this reduced set of genes, we further filtered down to only those results that had at least suggestive evidence ($p < 0.05$) of interaction between Ov and Ov-HRT treatment.

Differential exon usage (DEU) analysis

The DEXSeq pipeline was applied (with the default parameters) to analyze the aligned reads and obtain exon-level counts [66]. The exon-level counts were loaded and inspected in R (4.1.1) as DEXSeq objects before being normalized with DESeq2's normalization algorithm [64]. DEXSeq, similar to DESeq2, computes negative binomial regression and shares dispersion estimation across features. The program is designed to estimate differences in exon usage within a particular gene across conditions and will not identify genes with global differences in exon expression across a given gene (i.e., the genes identified by DEU analysis will be different than those identified in the DE analysis). We computed a model where the predictors included a dummy variable for the exon, an indicator variable for whether the animal had undergone Ov, as well as the interaction between the two to assess DEU age associated with Ov. A Benjamini–Hochberg FDR was applied to the unadjusted *p*-value to account for multiple comparisons [65]. Results with an FDR-adjusted $p < 0.05$ were retained for pathway analysis. Top results were also overlapped with DMR genes to assess whether changes in methylation appeared to be affecting the exon usage of any genes.

Genome-wide DNA methylation profiling

Genomic DNA was checked for quality by electrophoresis on a 0.7% agarose gel, using a NanoDrop 8000 spectrophotometer (Thermo Scientific, Wilmington, DE, USA) and quantified using a Qubit (Thermo Scientific, Wilmington, DE, USA). A total of 50 ng

of genomic DNA was sheared using a Bioruptor UCD200 (Diagenode, Denville, NJ, USA), generating fragments of ~ 180 bp. The Illumina TruSeq Methyl Capture EPIC library prep kit (Illumina, Santa Clara, CA, USA) was used following the manufacturer's instructions. The EPIC probes interrogate > 3.3 million individual CpG sites per sample at a single-nucleotide resolution. After end repair, 3′ A-tailing, and adaptor ligation, libraries were pooled in groups of four, followed by two rounds of hybridization and capture using the EPIC probes, bisulfite conversion, and final amplification. After library quantification using a 2100 Bioanalyzer (Agilent Technologies), DNA libraries were sequenced (3 libraries per 150PE lane) on an Illumina HiSeq4000 at the University of Oregon Genomics and Cell Characterization Core Facility (GC3F). Subsequently, 5% PhiX DNA (Illumina Inc.) was added to each library pool during cluster amplification to boost diversity. Cases and control samples were mixed within lanes and sequenced together on the same flow-cell to reduce the impact of batch effects on data. The quality of the bisulfite-converted sequencing reads was assessed with FastQC [61]. Reads were trimmed and aligned to the macaque reference genome (Mmul10), and then the bisulfite conversion rates were evaluated, insuring all libraries were > 98% converted, and CpG methylation was evaluated using Bismark [67]. The methylation rates were calculated as the ratio of methylated reads over the total number of reads. Methylation rates for CpGs with fewer than 10 reads were excluded from further analysis. We next removed CpG sites on sex chromosomes. The remaining ~ 2.8 to 3.0 million CpGs per sample (OC and PFC, respectively) post-filtering were used for downstream analyses.

The differential methylation analysis was carried out by applying a generalized linear mixed effects model (GLMM) implemented in R package PQLseq (version 1.2.1) [68, 69] separately for each CpG site. PQLseq models the technical sampling variation in bisulfite sequencing data with a binomial distribution. The methylation values were modeled as the outcome, and the predictor was whether or not an animal had undergone Ov. The relatedness of the animals was accounted for by modeling the relatedness as random effects, and for the test of interaction, we also modeled Ov-HRT status as an additional predictor and computed the interaction between Ov and Ov-HRT. Consistent with what was done with the gene expression data, the OI samples were replicated and relabeled with Ov-HRT and non-Ov-HRT categories to allow for the test of interaction. The most common methylation proportion values are 0 and 1, which are problematic in the context of generalized linear models with the logit link function (infinite in the logit-transformed space). We used a common pseudo-count transformation to avoid both extremes, as recommended, for example, by the developers of PQLseq [70]. This was done after adding + 1 to the number of methylated reads and + 2 to the total number of reads to avoid modeling methylation proportions that are exactly 0 or 1, as recommended by the authors of PQLseq [70]. This pseudo-count transformation was only applied to non-missing values (coverage > 10 ×).

Each nominal *p*-value was corrected for multiple comparisons by the Benjamini–Hochberg FDR [65]. In parallel, the nominal *p*-value was used as input for Comb-p [71] analysis to identify differentially methylated regions (DMRs) between OI, Ov, and Ov-HRT as previously described [72]. The Comb-p method uses a sliding window correction where each Wilcoxon *p*-value is adjusted by applying the Stouffer–Liptak–Kechris (slk) method [73–75] of neighboring *p*-values as weighted according to the observed autocorrelation (ACF) at the appropriate lag. Briefly, Comb-p calculates the ACF at varying distance lags, and then the ACF is used to perform the slk correction where each *p*-value is adjusted according to adjacent *p*-values as weighted according to the ACF. Thus, a given *p*-value will be pulled lower if its neighbors also have low *p*-values and likely remain insignificant if the neighboring *p*-values are also high. Next, a *q*-value score based on the Benjamini–Hochberg FDR correction is calculated. The peak-finding algorithm is used to find enrichment regions. Once the regions are identified, a *p*-value for each region can be assigned using the Stouffer–Liptak correction. Then, the false discovery rate *q*-value is used to define the extent of the region, whereas the slk-corrected *p*-value and the one-step Sidak multiple-testing correction [76] are used to define the significance of the region. Parameters for Combwere DIST = 300, STEP = 60, and THRESHOLD = 0.05.

Network analysis

Significant DMRs that had gene annotations, as well as DE genes and genes demonstrating DEU, were combined for each brain region. Those gene

lists were again combined across brain regions to identify significantly altered genes that replicated across both OC and PFC. Genes that were DE in both tissues were only retained if they were altered in consistent directions across both brain regions.

Results were analyzed in KEGG, STRING, and MCODE to find biological pathways enriched between groups (Fig. 2; Figs. S2 and S3) [77, 78]. STRING was used to obtain protein–protein interactions for all genes that met our filtering criteria for each omic analysis. STRING was applied to find only "high confidence" protein–protein interactions with options for "text mining" and "neighborhood" disabled [77]. MCODE was applied to the remaining interactions to obtain a set of highly interconnected gene clusters [78], and the biological functions of each cluster with MCODE scores greater than 4.0 were identified through the KEGG pathways [79].

Functional promoter/enhancer assay

To determine the promoter or enhancer activity capacity of two DMRs located in the promoter and overlapping with exon 1 of the rhesus macaque *LTBR* and overlapping with the last exon of *MZF1* and in the promoter of *UBE2M* genes, we cloned the corresponding macaque DMR regions (*LTBR* (PFC), chr11:6,528,520–6,529,383; *UBE2M* (PFC), chr19:58,128,610–58,130,108; and (OC), chr19: 58,128,532–58,130,175) in the luciferase reporter vector pGL3 (Promega) and transfected HEK293 cells (HEK 293, obtained from the Wake Core Repository). In addition, we transfected cells with the basic and control pGL3 as negative and positive controls; respectively. HEK293 cells were seeded in 96-well plates at 10,000 cells/well density and cultured in Dulbecco's modified Eagle medium (DMEM) containing high glucose (4.5 g/L) supplemented with 10% fetal bovine serum (FBS) and maintained at 37 °C and 5% CO_2. Twenty-four hours later, cells were transfected using 90 ng of each corresponding vector diluted in 10 µL of opti-medium and 0.3 µL of X-treme GENE HP DNA Transfection Reagent (Roche). Subsequently, 10 ng of Renilla vector (Promega) was co-transfected and used for normalization. After 48 h of transfection, Dual-Glo® reagent equal

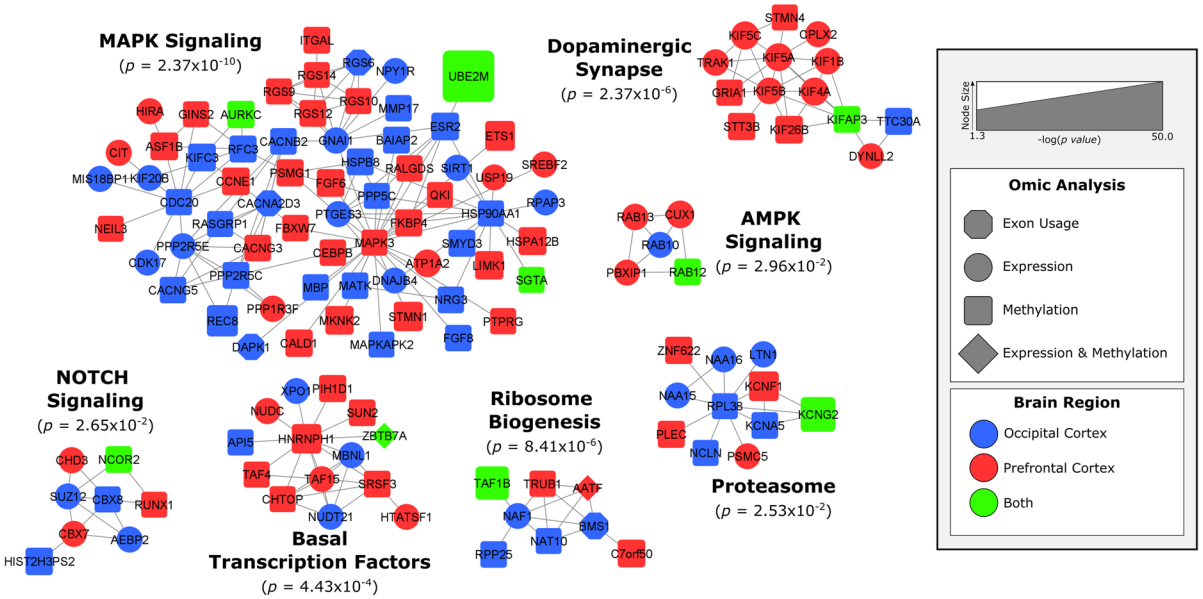

Fig. 2 Biological networks of ovariectomy-related changes in gene expression and DNA methylation. Protein interactions were obtained from STRING's protein interaction database. MCODE was used to find tightly connected clusters of interactions that are labeled according to functions defined in Gene Ontology biological processes (enrichment *p*-value listed). The color of the nodes reflects the tissue where the gene was identified while the shape of the nodes reflects which omics analysis the gene was identified in. The size of the node reflects statistical significance with larger nodes, like *UBE2M*, being more significant

to the volume of culture medium was added to each well. After 10 min, firefly luminescence was measured in a luminometer (SpectraMax iD3).

Results

Differential expression analysis

In the OC, 14,842 genes met the filtering criteria while 14,590 genes met the filtering criteria in the PFC. After computing association testing with each gene from each of those sets, we identified 150 and 128 differentially expressed (DE) genes associated with Ov (FDR < 0.05) in the OC and PFC, respectively (Table S1).

To explore if Ov-HRT treatment modulates the effect of Ov, we computed an interaction test between Ov-HRT treatment and Ov status. Instead of globally testing for an interaction between Ov-HRT and Ov status, we were primarily interested in genes that showed significant expression changes related to Ov that no longer showed a statistical association with Ov once the animals received Ov-HRT treatment. To obtain a general set of genes that fit this criterion, we filtered the results to include only genes that showed suggestive evidence of Ov association (unadjusted $p < 0.05$) without Ov-HRT treatment and little evidence of Ov association with Ov-HRT treatment (unadjusted $p > 0.1$). From this reduced set of 884 (PFC) and 663 genes (OC), we further filtered down to only those results that had suggestive evidence ($p < 0.05$) of interaction between Ov and Ov-HRT treatment. In the OC and PFC, we identified 19 and 10 genes, respectively, with suggestive evidence for Ov-HRT effects (Table 1). Ten of these genes are known to interact with the estrogen receptors or their expression being associated with the levels of estrogen. These include the transient receptor potential vanilloid 6 (*TRVP6*), adrenomedullin (*ADM*), the glucose transporter 12 (*SLC2A12*), supervillin (*SVIL*), acyl-CoA synthetase 2 (*ACSF2*), lymphotoxin-B receptor (*LTBR*), the hematopoietic PBX-interacting protein 1 (*PBXIP1*), the fucosyltransferase 1 (*FUT1*), neuromedin U (*NMU*), and the Purkinje cell protein 4 (*PCP4*). Furthermore, *TRVP6* is known to contain estrogen-responsive elements in its promoter. In the OC-specific network, *ADM* was part of the insulin secretion pathway. And in the OC/PFC combined network, *PBXIP1* was a member of the AMPK signaling pathway.

Differential exon usage analysis

These represent a unique set of genes that are being alternatively spliced in Ov animals and are mutually exclusive from the set of DE genes. Among these genes, *HADHB*, *MDH2*, and *ELMO1* are known to interact with ERs and/or have EREs (i.e., *ELMO1*). No exons were identified as significant in the test of interaction between Ov and Ov-HTR after correction for a FDR. Given the massive number of tests computed, the smaller sample size of the study, and the additional degrees of freedom needed to test the interaction between exon and Ov status (see "Methods" section), it is likely that we are underpowered to compute DEU analysis at this scale. Nonetheless, the 15 unique genes demonstrating significant DEU were included in the network analysis (Fig. 2). *BMS1*, *CACNA2D3*, *DAPK1*, and *RGS6* clustered into the MAPK signaling and ribosome biogenesis networks (Fig. 2). In addition, we overlapped each of the 15 DEU genes with significant DMRs in the OC (FDR < 0.05 and Sidak < 0.05) because exon usage can often be influenced by DNAm. We did not identify any overlapping results between the genes that were mapped to our significant DMRs and the DEU genes.

Differential methylation analysis

In the OC and PFC, 2.6 million and 2.9 million CpGs met the filtering (no missing values across samples and standard deviation of CpG methylation rate across all samples less than 5%), respectively. After computing association testing with each CpG from each of those sets, and aggregating the CpG results into DMRs, we identified 254 (OC) and 457 (PFC) significant (Sidak's $p < 0.05$) DMRs associated with Ov (Table S1). 24 DMRs were shared across both brain regions (Table 2). All of them showed the same direction of change in DNAm, except for the E3 ubiquitin-protein ligase, *TRIM36*, and the SH3-binding kinase 1, *SBK1*, that were hypomethylated in OC. Furthermore, *SBK1* is both hypermethylated and downregulated in the PFC. In the PFC, 5 DMRs showed overlap with DE genes (Table 2). The *UBEM2* (ubiquitin-conjugating enzyme 2) DMR is

Table 1 Interaction results. Genes that demonstrate suggestive evidence ($p < 0.05$) for a modifying estradiol result

Ensembl gene symbol	Gene name	Ov log2FC	Ov *p*	Ov-HRT log2FC	Ov-HRT *p*	Interaction *p*	Tissue
ENSMMUG00000008260	*P2RX1**	−1.65	6.10E-05	0.37	5.81E-01	9.64E-04	OC
ENSMMUG00000016219	*TRPV6*	0.93	1.58E-02	−0.43	4.67E-01	2.00E-03	OC
ENSMMUG00000049314	*DUSP2*	0.61	1.27E-02	−0.13	6.35E-01	2.46E-03	OC
ENSMMUG00000015308	*CAPN6*	−0.92	2.95E-02	0.96	6.39E-02	3.03E-03	PFC
ENSMMUG00000020213	*LTBR*	−0.72	2.90E-03	0.18	6.06E-01	4.09E-03	OC
ENSMMUG00000011426	*TIMP1*	−0.40	2.97E-02	0.23	1.66E-01	4.16E-03	PFC
ENSMMUG00000063192	*SOX17*	−0.98	8.29E-03	0.08	8.63E-01	7.62E-03	OC
ENSMMUG00000000662	*GBP3*	−0.43	6.81E-03	0.45	1.51E-01	1.10E-02	PFC
ENSMMUG00000007604	*PODN*	−0.77	2.92E-02	0.52	3.32E-01	1.14E-02	OC
ENSMMUG00000016387	*ADM*	0.61	4.31E-02	−0.18	5.82E-01	1.29E-02	OC
ENSMMUG00000016027	*SERTAD1*	0.49	3.25E-02	0.02	9.32E-01	1.63E-02	OC
ENSMMUG00000017327	*SLAMF7*	−1.72	1.62E-02	0.35	6.04E-01	1.79E-02	PFC
ENSMMUG00000022921	*SLC2A12*	−0.44	1.41E-02	0.06	7.74E-01	1.81E-02	OC
ENSMMUG00000002422	*AEBP1*	−0.93	5.65E-03	0.43	3.82E-01	2.63E-02	OC
ENSMMUG00000047632	*NA*	3.69	1.94E-03	1.44	6.97E-02	2.71E-02	OC
ENSMMUG00000001545	*NA*	0.64	1.22E-02	−0.02	9.47E-01	2.94E-02	OC
ENSMMUG00000020346	*CPXM2*	−1.15	3.70E-03	0.24	5.62E-01	2.99E-02	OC
ENSMMUG00000025057	*SNORD14*	0.70	3.37E-02	−0.30	4.81E-01	3.10E-02	PFC
ENSMMUG00000064609	*LIN28B*	0.87	1.51E-03	0.11	7.45E-01	3.15E-02	PFC
ENSMMUG00000022741	*WFIKKN2*	−0.94	7.49E-03	0.07	8.89E-01	3.33E-02	OC
ENSMMUG00000001374	*SVIL*	−0.47	2.61E-02	0.13	6.37E-01	3.56E-02	OC
ENSMMUG00000017236	*ACSF2*	−0.31	2.90E-02	0.19	4.00E-01	3.58E-02	PFC
ENSMMUG00000020213	*LTBR**	−0.86	1.90E-04	−0.04	9.01E-01	3.59E-02	PFC
ENSMMUG00000006576	*PBXIP1**	−0.59	1.35E-04	−0.12	5.76E-01	4.08E-02	PFC
ENSMMUG00000004020	*FUT1*	0.58	4.57E-02	−0.12	6.88E-01	4.19E-02	OC
ENSMMUG00000043692	*NMU*	1.30	1.41E-03	0.36	1.74E-01	4.21E-02	OC
ENSMMUG00000041181	*PCP4*	0.72	3.37E-02	−0.05	8.57E-01	4.36E-02	OC
ENSMMUG00000000984	*VILL*	1.07	1.81E-02	0.21	5.86E-01	4.51E-02	OC
ENSMMUG00000017360	*NT5DC2*	−0.30	3.20E-02	0.19	4.20E-01	4.54E-02	PFC

Genes in bold were differentially expressed and/or differentially methylated across brain areas

FC fold change, *Ov* ovariectomized, *Ov-HRT* ovariectomiced with hormone replacement therapy, *PFC* prefrontal cortex, *OC* occipital cortex

very strongly replicated across both brain regions, which again suggests this is unlikely to be a false positive (Fig. 3). *UBE2M* also shows suggestive evidence of differential expression in the OC (Fig. 3). In this case, the DMR (OC, 157 DMCs; PFC, 145 DMCs) is hypomethylated in both brain areas with Ov as compared to OI, and the gene is upregulated in the OC of Ov with or without HRT. The DMR is located ~ 3 kb upstream of the *UBE2M* transcription start site and mapping to the last exon of the *MZF1* gene. Differential expression was detected for *UBE2M* but not for the *MZF1* gene. According to the reporter assay results, the subregion within this DMR has promoter activity (Fig. S1), as shown by an increased luciferase relative light units (RLUs) as compared to the control vectors (PGL3 enhancer vector, Fig. S1).

To explore if Ov-HRT treatment modulates the effect of Ov, we also computed an interaction test between Ov-HRT treatment and Ov status. As expected for the sample size and the nature of combining CpGs to build DMRs, FDR adjustment left no DMRs. *LTBR*, as mentioned above, is a DE gene that is also a significant DMR in the PFC (Fig. 4). The DMR contains 57 DMCs and maps to

Table 2 Overlapping results. Genes that demonstrate either differential expression or methylation across both the occipital cortex and the prefrontal cortex with ovariectomy

Gene name	Occipital cortex			Prefrontal cortex		
	Effect	Adjusted *p*	Dataset	Effect	Adjusted *p*	Dataset
UBE2M	−0.17	1.65E-51	DMR	−0.13	9.63E-32	DMR
PLD6	−0.16	1.16E-20	DMR	−0.11	5.08E-03	DMR
KCNG2	−0.08	4.74E-19	DMR	−0.05	1.33E-08	DMR
RNF157	−0.14	5.94E-12	DMR	−0.42	1.34E-02	DEG
PPIAL4G	−0.15	9.66E-11	DMR	−0.24	5.36E-15	DMR
PTPRU	0.24	2.43E-06	DMR	0.11	7.68E-11	DMR
CHSY1	0.10	4.88E-05	DMR	0.08	8.27E-05	DMR
STX2	−0.06	6.29E-05	DMR	−0.13	2.70E-03	DMR
TRIM36	−0.95	2.78E-04	DEG	0.12	1.03E-02	DMR
KLK4	0.16	8.52E-04	DMR	0.09	1.44E-03	DMR
NCOR2	−0.08	1.11E-03	DMR	−0.08	1.37E-03	DMR
SBK1	−0.10	1.19E-03	DMR	0.10	1.54E-05	DEG & DMR
KIFAP3	0.03	1.35E-03	DMR	0.05	8.88E-03	DMR
GAS6	−0.22	2.77E-03	DMR	−0.06	8.21E-03	DMR
HAPLN4	0.15	3.58E-03	DMR	0.10	2.02E-04	DMR
RAB12	−0.13	5.24E-03	DMR	−0.08	1.90E-03	DMR
TAF1B	0.11	6.58E-03	DMR	0.12	1.84E-16	DMR
ADGRD1	0.10	7.40E-03	DMR	0.10	2.84E-03	DMR
SGTA	0.07	1.73E-02	DMR	0.09	3.24E-02	DMR
ZBTB7A	−0.12	2.30E-02	DMR	−0.83	3.62E-02	DEG
CEP170	−0.58	3.98E-02	DEG	−0.15	4.78E-24	DMR
AURKC	0.16	4.21E-02	DMR	0.10	6.35E-05	DMR
NUDT10	0.82	4.29E-02	DEG	1.00	3.82E-02	DEG
MEIS2	−0.11	4.94E-02	DMR	−0.09	1.76E-02	DMR

"Effect" stands for either a $\log_2$(fold-change) or a difference in methylation rates. A positive effect is indicative of an increase with ovariectomy, while a negative effect indicates a decrease with ovariectomy. "Adjusted *p*" is the *p*-value adjusted for multiple comparisons, either an FDR adjustment for DEGs or Sidak's adjustment for DMRs. For results that are both a DEG and a DMR in the same tissue, the DMR effect and *p*-value are listed

DMR differentially methylated region, *DEG* differentially expressed gene

the promoter and the first alternative exons of this gene. The DMR is significantly hypermethylated in Ov samples as compared to OI samples (average DNAm = 27% vs 14%; respectively), while in Ov-HRT, the methylation level was not different to OI or Ov (average DNAm = 20%). The promoter/enhancer assays and the position of the DMR suggest that this DMR is functioning as a promoter (Fig. S1). In agreement with this DMR functioning as a promoter, we observed a downregulation of *LTBR* with the hypermethylated DMR in Ov (Fig. 4), while the expression in OI and Ov-HRT did not differ.

Network analysis

Network analysis for each brain region was completed independently for each tissue. In the OC, we identified 150 DE genes and 254 DMRs, while we identified 128 DE genes and 457 DMRs significantly associated with Ov in the PFC (Table S1). In the OC, 23 genes clustered into 3 MCODE clusters (MCODE score > 4.0), and in the PFC, 48 genes clustered into 5 MCODE clusters (MCODE score > 4.0) (Figs. S2 and S3). Pathway analysis shows different pathways enriched in a tissue-specific manner, highlighting the particular function of each brain region. For instance,

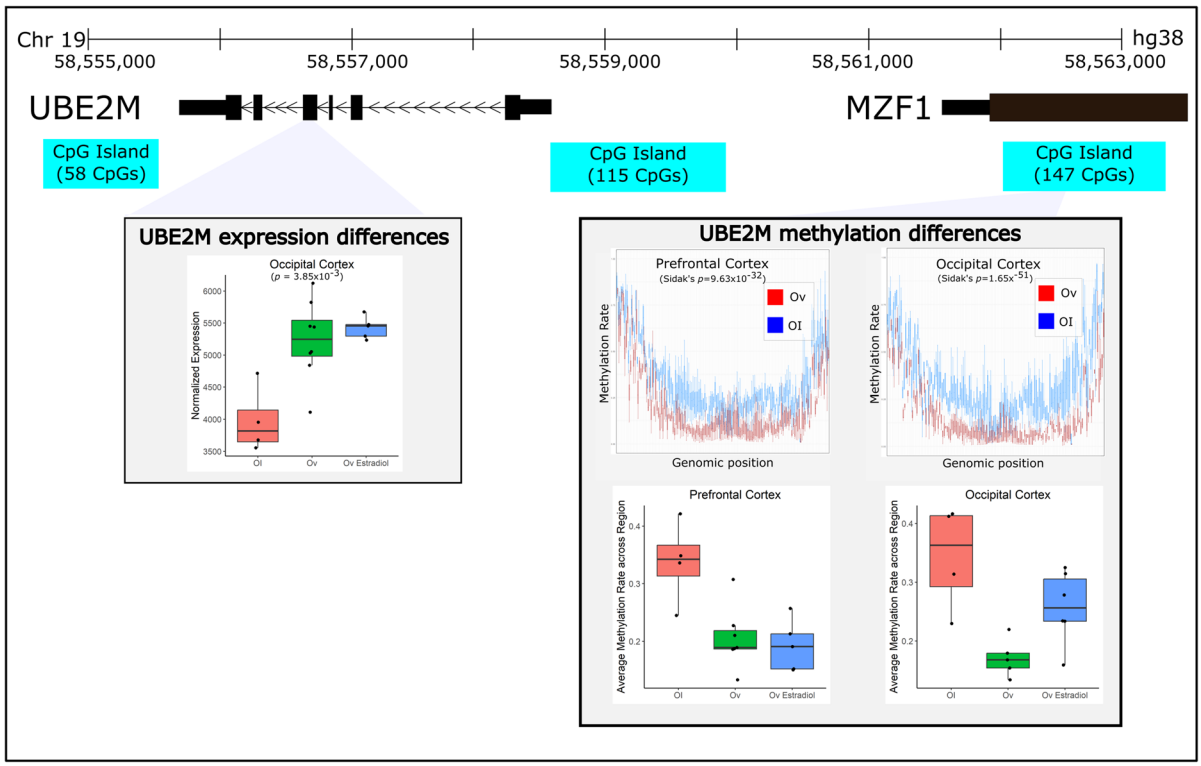

Fig. 3 Ovariectomy-related changes in gene expression and methylation of *UBE2M*. *UBE2M* was a gene that demonstrated significant differences in methylation across both brain regions. In addition, it demonstrated significant differences in expression in the OC. The DMR and CpG island that was annotated to *UBE2M* resides upstream of *UBE2M* in the same genomic region as the *MZF1* gene and appears to be hypo-methylated with ovariectomy. Expression of *UBE2M* increases with ovariectomy, regardless of E2 treatment, and average DNA methylation rates are not significantly altered with E2 treatment

in the OC, there was an enrichment in the regulation of insulin secretion, with *UBE2M* and *ADM* being hypermethylated and the estrogen receptor *ESR2* being hypomethylated in Ov. In the PFC, there was an enrichment in GPCR signaling, which included the pro-opiomelanocortin *POMC*, the G-protein signaling 17 (*RGS17*) or the G-protein subunit gamma 2 and 7 (*GNG2* and *GNG7*), among others. The ankyrin signaling pathway and the HSP90 chaperone-mediated activation of steroid hormone receptors were also enriched in the PFC with Ov. These pathways included *ANK1* and *ANK3*, several dyneins (*DYNLL2*, *DYNLT3*, and *DYNC1LI2*), and the FK506-binding protein 4 (*FKBP4*).

Given that the different brain regions under study play critical roles in processing cognitive functions, after filtering and manual curation to identify genes that were replicated across brain regions for omics, 891 total genes were submitted for global integrated network analysis (Fig. 2). Of the 891 genes, 127 genes clustered in 7 MCODE clusters (MCODE score > 4.0). The largest of the clusters contained 67 genes and was strongly enriched for "MAPK signaling". Genes with differential expression and methylation from both brain regions are similarly represented in this pathway. For instance, and within the regulators of the G-protein signaling (RGS) subcluster, all three members of the R12 family (*RGS10*, *12*, and *14*) were hypermethylated in Ov in the PFC. Exon 24 of the *RGS6* was downregulated in the OC leading to the production of different RGS6 transcripts under Ov conditions (Fig. S4). This brain specificity in the expression of RGS members may suggest activation/inhibition of different intracellular signaling cascades by brain region. One of the strongest results from the DNAm analyses, *UBE2M*, appears to play a key role in the regulation of this network (Fig. 2). *UBE2M* interestingly links into the pathway through the

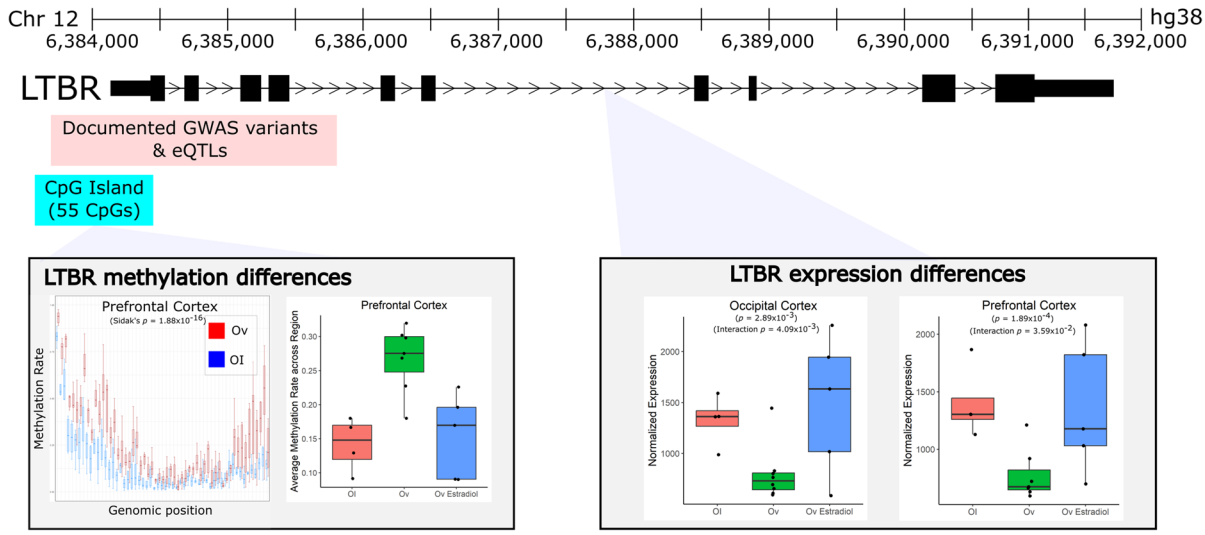

Fig. 4 Ovariectomy-related changes in gene expression and methylation of *LTBR*. *LTBR* was a gene that demonstrated differences in expression associated with ovariectomy across both brain regions. In addition, it demonstrated significant differences in methylation in the PFC (but no significant DMR was identified in the OC). The DMR and CpG island that was annotated to *LTBR* resides just upstream of *LTBR* and appears to be hypermethylated with ovariectomy. With average methylation rates, it appears that the hypermethylation in this region that is caused by Ov is modulated by estradiol treatment. The corresponding expression of *LTBR* decreases with ovariectomy but appears to be rescued to some degree with E2 treatment, particularly in the occipital cortex. Near the same region of the DMR lie a number of cis-acting eQTLs associated with *LTBR* expression that are also known GWAS variants for a variety of disorders—many of which are related to immune disorders

17β-estradiol receptor, *ESR2*, which is hypermethylated in Ov in the OC. Other key networks worth highlighting include those that were enriched for "AMPK signaling" and several signaling pathways involved in transcription and translation regulation (i.e., ribosome biogenesis; Fig. 2). Interestingly, an enrichment in "dopaminergic synapse" was, almost exclusively, found in the PFC. Within this network, the family of kinesin motor proteins, KIF, were primarily downregulated (*KIF5A-C*; *KIF1B*, *KIF4A*, *KIFAP3*) in Ov. Among this family, *KIF26B* was hypermethylated in Ov, but DNAm levels went down with Ov-HRT, more similar to the levels in OI.

Using the 29 genes from the interaction analysis across both brain regions, pathway enrichment suggests only two potential networks, HIF-1 signaling ($p = 0.0088$, *LTBR*, *TIMP1*) and neuroactive ligand-receptor interaction ($p = 0.0096$, *P2RX1*, *NMU*, *ADM*), suggesting that these genes and pathways may be working together in mediating the effects of HRT in Ov (Table 1).

Twenty-four genes showed overlap in consistent directions either across the two brain regions or both omics. These genes replicated across both regions or showed significant methylation and expression effects (Table 2). The network analysis highlights *UBE2M*, *AURKC*, *SGTA*, *RAB12*, *KIFAP3*, *NCOR2*, *TAF1B*, *ZBTB7A*, and *KCNG2* as genes with potentially key biological importance related to Ov across both brain regions (Fig. 2).

Discussion

Overall goals

This study examined the molecular effects of estrogen depletion at an older age on two different cortical regions, the OC and PFC, implicated in cognitive function. The OC controls visuospatial processing, distance and depth perception, color determination, object and face recognition, and memory formation [52, 53]. While the PFC is involved in working memory, temporal processing, decision-making, flexibility, and goal-oriented behavior [55]. Damage to these brain regions contributes to cognitive decline in dementia patients. While limited in sample size, this study leveraged an NHP model that was sufficiently

powered to detect significant differences in gene expression and DNAm because of our ability to tightly regulate the environment and obtain high-quality and highly reproducible brain samples. With this NHP model of middle-aged female rhesus macaques, we identified highly translatable molecular changes in the brain that are linked with the E2 depletion associated with Ov. Given the natural depletion of E2 that occurs with age, these results present a novel understanding of the role E2 plays in the aging brain and how long-term immediate HRT treatment (~4 years) can reverse or palliate those changes to maintain the brain in an age-matched molecular profile.

Because of the established relationship between E2 levels, its broad molecular regulatory function, and cognition [20, 30], we expected to identify robust molecular differences in these cognitive-relevant brain regions associated with Ov. For this reason, we completed RNA-sequencing to determine the genes that were DE and genome-wide DNAm sequencing to determine the genomic regions that were differentially methylated in the brains of animals that had undergone Ov for ~4 years prior to necropsy. As expected, we detected a large number of DMRs as well as DE genes—sometimes genes that were both DE and differentially methylated in their respective promoter/enhancer regions (Figs. 2 and 3, S1). We note, however, that because these results are derived from heterogeneous bulk tissue that contains many cell types, we are unable to attribute these differences to actual changes in the cell-type molecular mechanisms linked to Ov. Instead, it is possible that the changes we identify are driven by differences in the proportions of particular cell types. For example, *LTBR* is a gene that is primarily expressed in microglial cells. The differences we see in DNAm and expression between groups may either be attributed to a change in the abundance of microglia seen between groups or an actual shift in DNAm levels across cell types (or even just a large DNAm shift in microglia). A follow-up study using single-cell RNA-Seq would need to be completed to determine what the real drivers are in most of these cases.

Ov is associated with dramatic changes in neural signaling pathways

Pathway analysis revealed several networks of genes that changed with Ov (Fig. 2) in both brain regions. Importantly, all the identified networks had at least one gene that was DE and/or differentially methylated in both brain regions, suggesting a common link to the same pathways across them. These include the voltage-gated potassium channel encoded by *KCNG2* (proteasome, $p = 2.53 \times 10^{-2}$), the TATA-box-binding protein-associated factor (*TAF1B*, ribosome biogenesis, $p = 8.41 \times 10^{-6}$), the nuclear receptor corepressor 2 (*NCOR2*, NOTCH signaling, $p = 2.65 \times 10^{-2}$), the Ras-related protein 12 (*RAB12*, AMPK signaling, $p = 2.96 \times 10^{-2}$), and the kinesin-associated protein 3 (*KIFAP3*, dopaminergic synapse, $p = 2.37 \times 10^{-6}$). Interestingly, *KIFAP3* was downregulated in the PFC of Ov-HRT females under a chronic obesogenic diet [80]. In the current study, *KIFAP3* was hypermethylated in the PFC with Ov as compared to OI, while the DNAm levels were similar to the group receiving HRT. These results highlight the role of this gene in the PFC and its responsiveness to the presence of E2, independently of the diet. Within the basal transcription factors network ($p = 4.43 \times 10^{-4}$), the zinc finger and BTB domain-containing 7A factor (*ZBTB7A*) are known to transcriptionally upregulate ERα expression by directly binding to the *ESR1* promoter. In addition, ERα potentiates *ZBTB7A* expression via a positive loop in breast cancer [81]. In the PFC, *ZBTB7A* was downregulated, probably due to the absence of E2 in Ov, and, given the role of this transcription factor in metabolism [82], this downregulation could have implications in the regulation of brain metabolism.

The dopaminergic synapse pathway contained the *KIFAP3* gene which was hypermethylated in both brain regions and contained a number of other members of the kinesin heavy-chain proteins (i.e., *KIF1B*, *4A*, *5A*, *5B*, and *5C* were all downregulated in the PFC). Kinesins are molecular motors that transport cargo along microtubules [83]. These kinesin members are involved in transporting mitochondria, amyloid precursor protein vesicles, GABA and dopamine receptors, lysosomes, choline acetyltransferase, and dopamine [84–90]. Our results suggest that with Ov, there is a downregulation in kinesin expression that could be contributing to alterations in intracellular protein trafficking, for instance, dopamine receptors, that could impact synaptic function. A meta-analysis showed that AD patients had lower levels of dopamine and dopamine receptors (DRD1 and DRD2) as compared to controls, which could be contributing to dysregulation of mood and emotional stability as well as memory dysfunction [91].

One of the strongest biological pathways enriched in Ov was the MAPK signaling (enrichment $p = 2.3 \times 10^{-10}$). Prior evidence showed that E2 alters cellular components required for maintaining the balance between active and inactive MAPKs. For example, crosstalk between phosphorylation and ubiquitination pathways can exert long-term changes in cellular processes through multiple feedback loops that ultimately impact apoptosis and cell proliferation [92]. Among the members of the MAPK signaling pathway, the ERK 1 gene (*MAPK3*) and the ubiquitination gene *UBE2M* were hypomethylated, and several RGS proteins (*RGS 10*, *12*, and *14*) were hypermethylated in the PFC with Ov. Activation of ERK 1/2 subjected to G-protein-coupled receptor-mediated signaling is regulated through RGS proteins [93, 94]. Although additional studies analyzing protein levels and activation/inhibition ratio of these molecules are needed, our results suggest that RGS protein activity might be downregulated, leading to less inhibition of ERK 1, which would be consequently upregulated (supported by the hypomethylated DMR mapping to *MAPK3*). In addition, three genes are differentially methylated in both brain regions, *UBE2M*, *SGTA*, and *AURKC*. While little is known about the neural function of aurora kinase C (*AURKC*), the *SGTA* (small glutamine-rich tetratricopeptide-repeat-containing protein alpha) encodes for a molecular co-chaperone that interacts with steroid receptors and heat shock chaperone proteins, i.e., HSP90AA1 (Fig. 2), to regulate steroid receptor signaling, protein folding and conformation state, receptor stability, subcellular localization, and intracellular trafficking [95]. A study in yeast showed that Hsp90 functions to maintain the estrogen receptors in a high-affinity hormone-binding conformation [96]. Interestingly, *UBE2M* involvement in the MAPK signaling network is through its interaction with the ERβ gene (*ESR2*), that was hypermethylated in Ov (Fig. 2). Given its robust association with Ov across both brain regions and both the transcriptome and methylome, *UBE2M* is a strong result that should be heavily considered for further investigation. We confirmed that the DMR proximal to *UBE2M* functions as a promoter (Fig. S1), suggesting that changes in DNAm in this DMR may contribute to regulating its expression. Alterations in the ubiquitination system have been extensively linked to AD, with mutations in *UBB + 1* gene triggering neuronal degeneration [97, 98] and linked to spatial memory impairment [99]. UBE2M's primary function is as a ubiquitin-protein transferase, involved in protein neddylation, which is a post-translational ubiquitin-like protein modification that plays pivotal roles in protein quality control and homeostasis. Neddylation, involving UBE2M and other enzymes, is a critical mechanism for targeting and degrading misfolded or damaged proteins, helping to maintain protein quality control within brain cells [100]. For instance, during the initial stages of AD, ubiquitin–proteasome proteolysis degrades the abnormal amyloid β peptides and hyperphosphorylated tau. However, as the disease progresses, ubiquitination becomes ineffective at degrading the accumulating insoluble proteins [101], and neddylation seems to contribute to the degradation of these abnormal proteins. In AD patients, neddylation mechanisms are dysregulated [102], and neurons show accumulation of the neddylation enzyme NEDD8 in the cytoplasm and colocalization with ubiquitin and proteasome components in protein inclusions in the brain [102, 103]. Our results showed hypomethylation in both brain regions and upregulation of *UBE2M* in the OC. While additional studies are needed to determine the cellular localization of *UBE2M* and its role in protein neddylation, our results suggest that dysregulation of *UBE2M*, as well as the proteasome pathway (Fig. 2), that is associated with E2 depletion may be a key player mediating the negative effects that lack of E2 has on brain function [104]. In agreement with this hypothesis, our recently published analysis of the amygdala of these same females showed an increased accumulation of Aβ plaques in Ov females relative to those receiving E2 [105]. It remains to be determined wether similar differential expression of Aβ plaques also occurs in the OC and PFC. Together, these results emphasize *SGTA* and *UBE2M*, through their direct (*ESR2)* or indirect connections with the estrogen system, as critical mediators of a network of signaling pathways connected to protein degradation (i.e., proteasome and ubiquitination), synaptic function (i.e., dopamine), neuroinflammation, and neurodegeneration across brain regions [106–109].

Immediate estradiol supplementation ameliorates molecular alterations linked to Ov

After identifying molecular changes associated with Ov, we were interested in understanding whether

immediate (right after Ov) and long-term (over 4 years) E2 treatment reverse any of the changes linked to Ov. By identifying Ov-linked effects ameliorated by E2 treatment, the biological pathways that are directly impacted by estrogen levels become clearer. While E2 treatment ameliorates some of the behavioral and physiological changes seen following menopause in humans, the effects of E2 treatment on cognitive performance are still mixed [18]. Such inconclusive results could be due to the differences in HRT timing, diet, and other confounding variables common in human studies. Contrarily, results in NHPs on the beneficial effects of HRT on cognition are more consistent [30, 41], probably due to the controlled experimental conditions. For instance, a battery of behavioral testing conducted in the same females starting at 1 week following Ov and continuing for 12 months into the experimental design showed performance recovery in delayed response and visuospatial cueing tasks following E2 supplementation [30]. Thus, by understanding the specific genes altered by E2 in the brain with this animal model, we can begin to understand the biological pathways estrogen impacts and thereby develop more targeted therapeutics that specifically improve brain function and ultimately cognitive performance.

In the OC and PFC, we identified 19 and 10 genes, respectively, with suggestive evidence for E2 effects, where E2 appears to restore expression levels to a level that is similar to OI (Table 1). Among these 29 genes, the following are known to interact with the estrogen receptors, or its expression being associated with the levels of estrogen. *TRPV6* is a Ca^{2+}-selective channel that contains an ERE in its promoter [110], and its regulation by estrogen has been proposed in peripheral tissues [111] and the CNS, including the cortex [112]. TRPs participate in neurite outgrowth, receptor signaling, and excitotoxic cell death in the CNS. Furthermore, in mice, hypothalamic levels of Trpv6 are susceptible to estradiol oscillations through the estrous cycle, with higher Trpv6 levels at the proestrous phase where estrogen levels are at their highest [112]. Upregulation of intracellular Ca^{2+} and elevated Ca^{2+} influx via voltage-dependent Ca^{2+} channels have been reported to cause age-related alterations in neuronal activation. The diverse functions of neurons are dependent on Ca^{2+} signaling, which is influenced by the influx of Ca^{2+} from the extracellular environment or the release of Ca^{2+} from intracellular stocks in the endoplasmic reticulum. The concentration of Ca^{2+} in the cytosol is relatively low at the resting stage but shows a gradual increase after activation [113]. However, sustained intracellular Ca^{2+} disturbances are immediate causes of neurodegenerative diseases [114]. *TRPV1* has been associated with inflammation in AD; however, no information on the role of *TRPV6* in aging is available. In the OC, *TRPV6* was upregulated with Ov, and the levels decreased with HRT. These results disagree with previously reported findings in the hippocampus [112] and could stem from brain region–specific differences in *TRPV6* regulation. Nonetheless, our results suggest that without E2, there is an upregulation in *TRPV6*, and given its higher permeability to Ca^{2+} [115], this could lead to neuroinflammation. Importantly, E2 supplementation returns these levels to those of age-matched controls.

Adrenomedullin (*ADM*) is a peptide exerting important functions in the periphery and CNS. In the uterus, studies revealed that ADM promoter is recognized by the ER in a ligand-dependent manner and that there is a positive correlation between estrogen levels and *ADM* gene expression [116–119]. In the CNS, ADM is widely expressed through the brain [120], and its plasma levels increase with normal aging [121]. ADM is known to contribute to the activation of the hypothalamic–pituitary–adrenal (HPA) axis through the release of CRH [122], thus contributing to regulating hormonal responses to stress. Moreover, it acts as a neuromodulator through mechanisms dependent and independent of NMDA receptors [123]. In the brain of AD patients and in mouse models of AD, ADM seems to be associated with activated astrocytes in the vicinity of Aβ plaques [124, 125]. In the OC, *ADM*-relative expression levels increased after Ov, but its levels showed no significant differences from Ov-HRT, suggesting that a hypothetical reduction in Aβ plaques with E2 would then result in lower ADM levels.

AD is characterized by cerebral glucose hypometabolism. Glucose transporters are integral membrane proteins responsible for moving glucose from the bloodstream into cells. Extensive evidence has shown that non-vascular glucose transporters are altered in AD brains, causing glucose starvation and accelerated cognitive decline. In breast cancer cell lines, the insulin-sensitive glucose transporter 12 (*SLC2A12*) protein levels are increased with E2 [126], suggesting

a regulatory effect of estradiol on glucose metabolism. In the OC, *SLC2A12* (or *GLUT12*), which is expressed in cortical astrocytes [127], was found to be downregulated with Ov but normalized after E2 treatment. These results suggest that the lack of E2 may lead to glucose dysregulation and impairment in cognitive function. In addition to using glucose as an energy source, intracellular glucose is used for N-linked glycan biosynthesis, which is an understudied part of neural glucose metabolism. These N-glycans are terminal modifications in proteins (i.e., voltage-gated ion channels) that are required for protein function, from regulating action potential, neurotransmitter release, and synaptic transmission [128, 129], through the turnover and stability of brain glycoproteins such as synapsin 1[130]. The fucosyltransferase 1 (*FUT1*), which expression is mediated by the E2 [131], is one of the glycosylation enzymes that are required for synapse formation and neurite outgrowth. Global changes in N-linked glycoprotein profiles have been identified in CSF from AD patients, leading to its potential use as a biomarker for AD progression [132]. In our study, *FUT1* was upregulated in the OC with Ov, but normalized in Ov-HRT; suggesting that Ov may be associated with aberrations in the N-glycoproteome.

Neuromedin U (*NMU*) is a gonadal peptide, which receptor, neuromedin U2 is expressed throughout the brain [133]. It is suggested that *NMU* has a protective role in neurodegenerative diseases [134]. In particular, *NMU* protects neuronal cell viability and inhibits inflammation-induced memory impairments [134]. Others have shown that estradiol levels following Ov in rats resulted in alterations in *NMU* levels in the brain [135, 136]. Although this effect seems to be estradiol dose-dependent, with low estradiol levels increasing *NMU* expression levels, this increment was only previously observed with progesterone supplementation [135, 136]. Our results show the same trend, with higher levels of *NMU* in Ov, but lower levels in the group receiving E2. A possible explanation for these results could be that if there is higher neuroinflammation with Ov, NMU might be upregulated to counteract that inflammation.

The Purkinje cell protein 4 (*PCP4*) is a calmodulin-binding anti-apoptotic peptide in neural cells and an estrogen-inducible peptide in breast cancer cell lines [137]. A recent study showed that *PCP4* was upregulated in transgenic mice, and *PCP4* promoted the synthesis of Aβ, increased Aβ deposition, plaque formation, affected Aβ protein precursor processing, and worsened learning and memory impairment in the transgenic AD mouse model [138]. Our results identified an upregulated *PCP4* in Ov, which would support the development of Aβ pathology, while Ov-HRT females had lower levels of *PCP4*, suggesting that E2 offers some protection.

The hematopoietic PBX-interacting protein 1 (*PBXIP1*) is a transcription factor involved in extracellular matrix organization and chromatin regulation. It is an ER-interacting protein that regulates estrogen-mediated breast cancer cell proliferation and tumorigenesis [139]. A recent integrative multi-omics analysis on the human PFC found *PBXIP1* being statistically associated with the three main neuropathological AD traits (extracellular Aβ plaques, phosphorylated-tau neuronal tangles, and their density). It has been suggested that these effects are mediated through *PBXIP1*'s role in astrocytes [140, 141] and hippocampal neurons where its expression is linked to *neuronal degeneration* in postmenopausal women [142]. Indeed, some studies have demonstrated that *PBXIP1* is a scaffolding protein that can bind ERs and regulate E2 signaling cascades [47, 50]. Short-term E2 treatment enhanced ER interaction with the *PBXIP1*–microtubule complex and resulted in cytoplasmic localization, while microtubule depolymerization disrupted the *PBXIP1*–ER–microtubule complex and increased ER nuclear transcriptional activity, suggesting that ER interaction with *PBXIP1* promotes cytoplasmic localization of ERs [25, 48, 51]. In our study, *PBXIP1* was downregulated by Ov (Fig. 2) but normalized in Ov-HRT, suggesting that when E2 is present in sufficient amounts, *PBXIP1* is critical to shuttling E2 between the nucleus and cytosol [48] so that E2 can exert its functions.

While the specific function of these genes in the cortex and how E2 is regulating their function remain to be investigated, our results indicate that Ov might be leading to neuroinflammation, Aβ plaque formation, and cognitive decline through glucose metabolism, intracellular Ca^{2+} levels, and microtubule and N-glycosylation disruptions, importantly. Ov-HRT treatment might delay/prevent AD-related pathology by altering the expression levels of these genes (and likely associated pathways) to normalize them to those levels of age-matched controls.

Enrichment analysis of these 29 DE genes revealed two small networks that were significant: HIF-1 signaling ($p=0.0088$, *LTBR*, *TIMP1*) and neuroactive ligand-receptor interaction ($p=0.0096$, *P2RX1*, *NMU*, *ADM*). HIF-1 signaling has been previously linked to estradiol [143] and has been shown to regulate neuroinflammation in traumatic brain injury [144]. This network contains the *LTBR*), which is one of our most promising results that demonstrates differential expression effects in both brain areas. We also identified a DMR mapping to *LTBR* in the PFC (Fig. 3). We confirmed that the DMR proximal to *LTBR* is a promoter (Fig. S2). LTBR has been mostly studied in lymphoid tissues, with data supporting its role as a regulator of inflammation [145], a process known to be modulated by estrogen as well [146]. In fact, LTBR signaling can activate both canonical and alternative NF-κβ signaling to induce proinflammatory chemokines and cytokines [147]. Although studies on the role of *LTBR* in brain function remain mostly unexplored, a recent transcriptomic study identified *LTBR* as a neuroinflammatory biomarker of AD [148]. More specifically, it has been recently shown that *LTBR* is upregulated in microglia of aged (mean age of 94 years) brains as compared to middle-aged (mean age of 53 years) human brains [149], which could suggest that upregulated *LTBR* levels might be mediating age-related neuroinflammation through microglial function. However, the relationship between *LTBR* expression/function and microglial activation status remains unknown, and additional studies are needed to determine how or whether *LTBR* mediates microglial activation. Others have shown that estrogen can inactivate microglia through the ERβ [150]. Our results show increased DNAm levels and decreased levels of *LTBR* expression with Ov (Fig. 3), with *LTBR* expression levels reverting to OI levels with HRT. As discussed earlier, it is possible that the changes in DNAm and gene expression seen with Ov-HRT are associated with a change in the proportions of cell types, namely microglia, with Ov-HRT. This is a limitation in this study, and we cannot exclude that such molecular changes are due to a change in the number of microglia present, their activation status, or a combination of all. Nonetheless, it is evident from our results that understanding the role of *LTBR* in microglia function would be of critical importance to understanding estrogen's relationship to brain function.

Conclusions

This work highlights the importance of multiple omics across multiple brain regions to identify robust molecular signals linked to E2 regulation in the aging brain. By including multiple omics and more than one brain area, we were able to home in on biological effects that replicated across brain regions and thereby reduce noise from false positives. Importantly, this work represents a major step toward understanding molecular changes in the brain that are linked to Ov and how HRT may revert or protect against the negative consequences of a depletion in E2. Our findings indicate that the molecular profile of the cortical regions (OC and PFC) in the absence of E2 may lead to neuroinflammation and neuropathology compatible with AD disease by the dysregulation of intracellular axonal protein trafficking, protein ubiquitination, glucose metabolism, intracellular Ca^{2+} levels, and microtubule and N-glycosylation disruptions that are necessary for proper function of brain cells. Immediate HRT reverted these effects, at least partially, by bringing the epigenetic/transcriptomic profile of genes involved in neuroinflammation and other unknown functions, to that profile of age-matched OI females. It remains to be known if the molecular profile of the brain after HRT is more similar to that of younger OI brains, which we are currently investigating. Nonetheless, our results present real opportunities to discover novel therapeutics to slow cognitive decline caused by the lack of E2. Although our work needs further validation with larger cohorts, it also requires focused investigations of some of the genes we identified with very robust effects like *LTBR* and *UBE2M*. Moreover, because our studies were performed in an NHP preclinical animal model of human aging, the findings may have more immediate translational potential for clinical studies involving postmenopausal women.

Author contribution SGK, HFU, and RCJ designed the experiments. SGK and HFU provided the rhesus macaque samples. RCJ isolated all the DNA and RNA samples and prepared all the omics libraries. DZ and JB conducted the reporter assays. DNA methylation and gene expression bioinformatic analyses were performed by KDZ and LJW, and KDZ advised and conducted the appropriate statistical analyses to be performed in all the experiments. SGK, HFU, KDZ, and RCJ wrote the manuscript with the help of all the authors.

Funding Open access funding provided by the Carolinas Consortium. National Institutes of Health Grants: P30 AG066518, P51 OD011092, and RF1 AG062220.

Data availability The data that support the findings of this study are available on SRA under the following accession number: PRJNA1088413.

Declarations

Competing interests The authors declare no competing interests.

References

1. Kuiper GG, Carlsson B, Grandien K, Enmark E, Haggblad J, Nilsson S, et al. Comparison of the ligand binding specificity and transcript tissue distribution of estrogen receptors alpha and beta. Endocrinology. 1997;138(3):863–70.
2. Kuiper GG, Gustafsson JA. The novel estrogen receptor-beta subtype: potential role in the cell- and promoter-specific actions of estrogens and anti-estrogens. FEBS Lett. 1997;410(1):87–90.
3. Bagger YZ, Tanko LB, Alexandersen P, Qin G, Christiansen C, Group PS. Early postmenopausal hormone therapy may prevent cognitive impairment later in life. Menopause. 2005;12(1):12–7.
4. Hogervorst E, Williams J, Budge M, Riedel W, Jolles J. The nature of the effect of female gonadal hormone replacement therapy on cognitive function in postmenopausal women: a meta-analysis. Neuroscience. 2000;101(3):485–512.
5. Yesufu A, Bandelow S, Hogervorst E. Meta-analyses of the effect of hormone treatment on cognitive function in postmenopausal women. Womens health (Lond). 2007;3(2):173–94.
6. Thomas P, Pang Y, Filardo EJ, Dong J. Identity of an estrogen membrane receptor coupled to a G protein in human breast cancer cells. Endocrinology. 2005;146(2):624–32.
7. Freeman EW, Sammel MD, Lin H, Gracia CR, Pien GW, Nelson DB, et al. Symptoms associated with menopausal transition and reproductive hormones in midlife women. Obstet Gynecol. 2007;110(2 Pt 1):230–40.
8. Gold EB, Colvin A, Avis N, Bromberger J, Greendale GA, Powell L, et al. Longitudinal analysis of the association between vasomotor symptoms and race/ethnicity across the menopausal transition: study of women's health across the nation. Am J Public Health. 2006;96(7):1226–35.
9. Kravitz HM, Janssen I, Bromberger JT, Matthews KA, Hall MH, Ruppert K, et al. Sleep trajectories before and after the final menstrual period in the study of women's health across the nation (SWAN). Curr Sleep Med Rep. 2017;3(3):235–50.
10. Lamar M, Resnick SM, Zonderman AB. Longitudinal changes in verbal memory in older adults: distinguishing the effects of age from repeat testing. Neurology. 2003;60(1):82–6.
11. Boulware MI, Heisler JD, Frick KM. The memory-enhancing effects of hippocampal estrogen receptor activation involve metabotropic glutamate receptor signaling. J Neurosci. 2013;33(38):15184–94.
12. Carrer HF, Araque A, Buno W. Estradiol regulates the slow Ca2+-activated K+ current in hippocampal pyramidal neurons. J Neurosci. 2003;23(15):6338–44.
13. Fugger HN, Kumar A, Lubahn DB, Korach KS, Foster TC. Examination of estradiol effects on the rapid estradiol mediated increase in hippocampal synaptic transmission in estrogen receptor alpha knockout mice. Neurosci Lett. 2001;309(3):207–9.
14. Kim MT, Soussou W, Gholmieh G, Ahuja A, Tanguay A, Berger TW, et al. 17beta-Estradiol potentiates field excitatory postsynaptic potentials within each subfield of the hippocampus with greatest potentiation of the associational/commissural afferents of CA3. Neuroscience. 2006;141(1):391–406.
15. Wong M, Moss RL. Electrophysiological evidence for a rapid membrane action of the gonadal steroid, 17 beta-estradiol, on CA1 pyramidal neurons of the rat hippocampus. Brain Res. 1991;543(1):148–52.
16. Wong M, Moss RL. Long-term and short-term electrophysiological effects of estrogen on the synaptic properties of hippocampal CA1 neurons. J Neurosci. 1992;12(8):3217–25.
17. Babayan AH, Kramar EA. Rapid effects of oestrogen on synaptic plasticity: interactions with actin and its signalling proteins. J Neuroendocrinol. 2013;25(11):1163–72.
18. Russell JK, Jones CK, Newhouse PA. The role of estrogen in brain and cognitive aging. Neurotherapeutics. 2019;16(3):649–65.
19. Phan A, Lancaster KE, Armstrong JN, MacLusky NJ, Choleris E. Rapid effects of estrogen receptor alpha and beta selective agonists on learning and dendritic spines in female mice. Endocrinology. 2011;152(4):1492–502.
20. Luine VN. Estradiol and cognitive function: past, present and future. Horm Behav. 2014;66(4):602–18.

21. Vina J, Lloret A. Why women have more Alzheimer's disease than men: gender and mitochondrial toxicity of amyloid-beta peptide. J Alzheimers Dis. 2010;20(Suppl 2):S527–33.
22. Zarate S, Stevnsner T, Gredilla R. Role of estrogen and other sex hormones in brain aging. Neuroprotection and DNA repair. Front Aging Neurosci. 2017;9:430.
23. Pike CJ. Sex and the development of Alzheimer's disease. J Neurosci Res. 2017;95(1–2):671–80.
24. Song YJ, Li SR, Li XW, Chen X, Wei ZX, Liu QS, et al. The effect of estrogen replacement therapy on Alzheimer's disease and parkinson's disease in postmenopausal women: a meta-analysis. Front Neurosci. 2020;14:157.
25. O'Brien J, Jackson JW, Grodstein F, Blacker D, Weuve J. Postmenopausal hormone therapy is not associated with risk of all-cause dementia and Alzheimer's disease. Epidemiol Rev. 2014;36(1):83–103.
26. Shumaker SA, Legault C, Rapp SR, Thal L, Wallace RB, Ockene JK, et al. Estrogen plus progestin and the incidence of dementia and mild cognitive impairment in postmenopausal women: the women's health initiative memory study: a randomized controlled trial. JAMA. 2003;289(20):2651–62.
27. Davey DA. Menopausal hormone therapy: a better and safer future. Climacteric. 2018;21(5):454–61.
28. Espeland MA, Rapp SR, Shumaker SA, Brunner R, Manson JE, Sherwin BB, et al. Conjugated equine estrogens and global cognitive function in postmenopausal women: women's health initiative memory study. JAMA. 2004;291(24):2959–68.
29. Khadilkar SS. Post-reproductive health: window of opportunity for preventing comorbidities. J Obstet Gynaecol India. 2019;69(1):1–5.
30. Kohama SG, Renner L, Landauer N, Weiss AR, Urbanski HF, Park B, et al. Effect of ovarian hormone therapy on cognition in the aged female rhesus macaque. J Neurosci. 2016;36(40):10416–24.
31. Paganini-Hill A, Henderson VW. Estrogen deficiency and risk of Alzheimer's disease in women. Am J Epidemiol. 1994;140(3):256–61.
32. Rapp SR, Espeland MA, Shumaker SA, Henderson VW, Brunner RL, Manson JE, et al. Effect of estrogen plus progestin on global cognitive function in postmenopausal women: the women's health initiative memory study: a randomized controlled trial. JAMA. 2003;289(20):2663–72.
33. Rocca WA, Grossardt BR, Shuster LT. Oophorectomy, estrogen, and dementia: a 2014 update. Mol Cell Endocrinol. 2014;389(1–2):7–12.
34. Scheyer O, Rahman A, Hristov H, Berkowitz C, Isaacson RS, Diaz Brinton R, et al. Female sex and Alzheimer's risk: the menopause connection. J Prev Alzheimers Dis. 2018;5(4):225–30.
35. Shao H, Breitner JC, Whitmer RA, Wang J, Hayden K, Wengreen H, et al. Hormone therapy and Alzheimer disease dementia: new findings from the Cache County study. Neurology. 2012;79(18):1846–52.
36. Brann DW, Lu Y, Wang J, Sareddy GR, Pratap UP, Zhang Q, et al. Neuron-derived estrogen-a key neuromodulator in synaptic function and memory. Int J Mol Sci. 2019;39(15):2792–809.
37. Lu Y, Sareddy GR, Wang J, Wang R, Li Y, Dong Y, et al. Neuron-derived estrogen regulates synaptic plasticity and memory. J Neurosci. 2019;39(15):2792–809.
38. Brzozowska M, Lewinski A. Changes of androgens levels in menopausal women. Prz Menopauzalny. 2020;19(4):151–4.
39. Jacoby VL, Grady D, Wactawski-Wende J, Manson JE, Allison MA, Kuppermann M, et al. Oophorectomy vs ovarian conservation with hysterectomy: cardiovascular disease, hip fracture, and cancer in the women's health initiative observational study. Arch Intern Med. 2011;171(8):760–8.
40. Downs JL, Urbanski HF. Neuroendocrine changes in the aging reproductive axis of female rhesus macaques (*Macaca mulatta*). Biol Reprod. 2006;75(4):539–46.
41. Baxter MG, Santistevan AC, Bliss-Moreau E, Morrison JH. Timing of cyclic estradiol treatment differentially affects cognition in aged female rhesus monkeys. Behav Neurosci. 2018;132(4):213–23.
42. Zimmerman B, Kundu P, Liu Z, Urbanski HF, Kroenke CD, Kohama SG, et al. Longitudinal effects of immediate and delayed estradiol on cognitive performance in a spatial maze and hippocampal volume in menopausal macaques under an obesogenic diet. Front Neurol. 2020;11:539.
43. Appleman ML, Nilaver BI, Weiss A, Kohama SG, Urbanski HF. Effect of hormone replacement therapy on amyloid beta (Aβ) plaque density in the rhesus macaque amygdala. Front Aging Neurosci. 2024;15:1326747.
44. Kovacs T, Szabo-Meleg E, Abraham IM. Estradiol-induced epigenetically mediated mechanisms and regulation of gene expression. Int J Mol Sci. 2020;21(9):3177.
45. Marino M, Galluzzo P, Ascenzi P. Estrogen signaling multiple pathways to impact gene transcription. Curr Genomics. 2006;7(8):497–508.
46. Thakur MK, Paramanik V. Role of steroid hormone coregulators in health and disease. Horm Res. 2009;71(4):194–200.
47. Zhang P, Li L, Bao Z, Huang F. Role of BAF60a/BAF60c in chromatin remodeling and hepatic lipid metabolism. Nutr Metab (Lond). 2016;13:30.
48. Ghosh S, Thakur MK. Interaction of estrogen receptor-alpha ligand binding domain with nuclear proteins of aging mouse brain. J Neurosci Res. 2009;87(11):2591–600.
49. Paramanik V, Thakur MK. Estrogen receptor beta and its domains interact with casein kinase 2, phosphokinase C, and N-myristoylation sites of mitochondrial and nuclear proteins in mouse brain. J Biol Chem. 2012;287(26):22305–16.
50. Vini R, Rajavelu A, Sreeharshan S. 27-Hydroxycholesterol, the estrogen receptor modulator, alters DNA methylation in breast cancer. Front Endocrinol (Lausanne). 2022;13:783823.
51. Zhao Z, Fan L, Frick KM. Epigenetic alterations regulate estradiol-induced enhancement of memory consolidation. Proc Natl Acad Sci USA. 2010;107(12):5605–10.
52. Rehman A, Al Khalili Y. Neuroanatomy, occipital lobe. Treasure Island: StatPearls; 2024.
53. Stufflebeam SM, Rosen BR. Mapping cognitive function. Neuroimaging Clin N Am. 2007;17(4):469–84.
54. Holroyd S, Shepherd ML, Downs JH 3rd. Occipital atrophy is associated with visual hallucinations in

Alzheimer's disease. J Neuropsychiatry Clin Neurosci. 2000;12(1):25–8.
55. Funahashi S, Andreau JM. Prefrontal cortex and neural mechanisms of executive function. J Physiol Paris. 2013;107(6):471–82.
56. Hwang J, Kim CM, Kim JE, Oh M, Oh JS, Yoon YW, et al. Clinical implications of amyloid-beta accumulation in occipital lobes in Alzheimer's continuum. Brain Sci. 2021;11(9):1232.
57. Jobson DD, Hase Y, Clarkson AN, Kalaria RN. The role of the medial prefrontal cortex in cognition, ageing and dementia. Brain Commun. 2021;3(3):fcab125.
58. Chiou KL, Montague MJ, Goldman EA, Watowich MM, Sams SN, Song J, et al. Rhesus macaques as a tractable physiological model of human ageing. Philos Trans R Soc Lond B Biol Sci. 2020;375(1811):20190612.
59. Roth GS, Mattison JA, Ottinger MA, Chachich ME, Lane MA, Ingram DK. Aging in rhesus monkeys: relevance to human health interventions. Science. 2004;305(5689):1423–6.
60. Gilardi KV, Shideler SE, Valverde CR, Roberts JA, Lasley BL. Characterization of the onset of menopause in the rhesus macaque. Biol Reprod. 1997;57(2):335–40.
61. Andrews S. FastQC: a quality control tool for high throughput sequence data. 2010.
62. Dobin A, Davis CA, Schlesinger F, Drenkow J, Zaleski C, Jha S, et al. STAR: ultrafast universal RNA-seq aligner. Bioinformatics. 2013;29(1):15–21.
63. Liao Y, Smyth GK, Shi W. featureCounts: an efficient general purpose program for assigning sequence reads to genomic features. Bioinformatics. 2014;30(7):923–30.
64. Love MI, Huber W, Anders S. Moderated estimation of fold change and dispersion for RNA-seq data with DESeq2. Genome Biol. 2014;15(12):550.
65. Benjamini Y, Hochberg Y. Controlling the false discovery rate: a practical and powerful approach to multiple testing. J R Stat Soc Ser B. 1995;57(1):285–300.
66. Anders S, Reyes A, Huber W. Detecting differential usage of exons from RNA-seq data. Genome Res. 2012;22(10):2008–17.
67. Krueger F, Andrews SR. Bismark: a flexible aligner and methylation caller for Bisulfite-Seq applications. Bioinformatics. 2011;27(11):1571–2.
68. R Development Core Team. R: a language and environment for statistical computing. 2010.
69. Sun S, Zhu J, Zhou X. Efficient mixed model analysis of count data in large-scale genomic sequencing studies. 2022. pp. 2–7.
70. Laajala E, Halla-Aho V, Gronroos T, Kalim UU, Vaha-Makila M, Nurmio M, et al. Permutation-based significance analysis reduces the type 1 error rate in bisulphite sequencing data analysis of human umbilical cord blood samples. Epigenetics. 2022;17(12):1608–27.
71. Pedersen BS, Schwartz DA, Yang IV, Kechris KJ. Comb-p: software for combining, analyzing, grouping and correcting spatially correlated p-values. Bioinformatics. 2012;28(22):2986–8.
72. Cervera-Juanes R, Wilhelm LJ, Park B, Grant KA, Ferguson B. Alcohol-dose-dependent DNA methylation and expression in the nucleus accumbens identifies coordinated regulation of synaptic genes. Transl Psychiatry. 2017;7(1):e994.
73. Kechris KJ, Biehs B, Kornberg TB. Generalizing moving averages for tiling arrays using combined p-value statistics. Stat Appl Genet Mol Biol. 2010;9:29.
74. Liptak T. On the combination of independent tests. Magyar Tudomanyos Akademia Matematikai Kutato Intezetenek Kozlemenyei. 1958;3:171–97.
75. Stouffer SA. The American soldier. Princeton, NJ: Princeton University Press; 1949.
76. Šidák Z. Rectangular confidence region for the means of multivariate normal distributions. J Am Stat Assoc. 1967;62:626–33.
77. Szklarczyk D, Gable AL, Nastou KC, Lyon D, Kirsch R, Pyysalo S, et al. The STRING database in 2021: customizable protein-protein networks, and functional characterization of user-uploaded gene/measurement sets. Nucleic Acids Res. 2021;49(D1):D605–12.
78. Bader GD, Hogue CW. An automated method for finding molecular complexes in large protein interaction networks. BMC Bioinformatics. 2003;13(4):2.
79. Kanehisa M, Sato Y, Kawashima M, Furumichi M, Tanabe M. KEGG as a reference resource for gene and protein annotation. Nucleic Acids Res. 2016;44(D1):D457–62.
80. Cervera-Juanes R, Darakjian P, Ball M, Kohama SG, Urbanski HF. Effects of estradiol supplementation on the brain transcriptome of old rhesus macaques maintained on an obesogenic diet. Geroscience. 2022;44(1):229–52.
81. Molloy ME, Lewinska M, Williamson AK, Nguyen TT, Kuser-Abali G, Gong L, et al. ZBTB7A governs estrogen receptor alpha expression in breast cancer. J Mol Cell Biol. 2018;10(4):273–84.
82. Ren R, Horton JR, Chen Q, Yang J, Liu B, Huang Y, et al. Structural basis for transcription factor ZBTB7A recognition of DNA and effects of ZBTB7A somatic mutations that occur in human acute myeloid leukemia. J Biol Chem. 2023;299(2):102885.
83. De Vos KJ, Grierson AJ, Ackerley S, Miller CC. Role of axonal transport in neurodegenerative diseases. Annu Rev Neurosci. 2008;31:151–73.
84. Cromberg LE, Saez TMM, Otero MG, Tomasella E, Alloatti M, Damianich A, et al. Neuronal KIF5b deletion induces striatum-dependent locomotor impairments and defects in membrane presentation of dopamine D2 receptors. J Neurochem. 2019;149(3):362–80.
85. Kamal A, Stokin GB, Yang Z, Xia CH, Goldstein LS. Axonal transport of amyloid precursor protein is mediated by direct binding to the kinesin light chain subunit of kinesin-I. Neuron. 2000;28(2):449–59.
86. Kanai Y, Okada Y, Tanaka Y, Harada A, Terada S, Hirokawa N. KIF5C, a novel neuronal kinesin enriched in motor neurons. J Neurosci. 2000;20(17):6374–84.
87. Nakajima K, Yin X, Takei Y, Seog DH, Homma N, Hirokawa N. Molecular motor KIF5A is essential for GABA(A) receptor transport, and KIF5A deletion causes epilepsy. Neuron. 2012;76(5):945–61.
88. Tanaka Y, Kanai Y, Okada Y, Nonaka S, Takeda S, Harada A, et al. Targeted disruption of mouse conventional kinesin heavy chain, kif5B, results in

abnormal perinuclear clustering of mitochondria. Cell. 1998;93(7):1147–58.
89. Twelvetrees AE, Yuen EY, Arancibia-Carcamo IL, MacAskill AF, Rostaing P, Lumb MJ, et al. Delivery of GABAARs to synapses is mediated by HAP1-KIF5 and disrupted by mutant huntingtin. Neuron. 2010;65(1):53–65.
90. Landers JE, Melki J, Meininger V, Glass JD, van den Berg LH, van Es MA, et al. Reduced expression of the kinesin-associated protein 3 (KIFAP3) gene increases survival in sporadic amyotrophic lateral sclerosis. Proc Natl Acad Sci USA. 2009;106(22):9004–9.
91. Pan X, Kaminga AC, Wen SW, Wu X, Acheampong K, Liu A. Dopamine and dopamine receptors in Alzheimer's disease: a systematic review and network meta-analysis. Front Aging Neurosci. 2019;11:175.
92. Nguyen LK, Kolch W, Kholodenko BN. When ubiquitination meets phosphorylation: a systems biology perspective of EGFR/MAPK signalling. Cell Commun Signal. 2013;31(11):52.
93. Anger T, Klintworth N, Stumpf C, Daniel WG, Mende U, Garlichs CD. RGS protein specificity towards Gq- and Gi/o-mediated ERK 1/2 and Akt activation, in vitro. J Biochem Mol Biol. 2007;40(6):899–910.
94. Leone AM, Errico M, Lin SL, Cowen DS. Activation of extracellular signal-regulated kinase (ERK) and Akt by human serotonin 5-HT(1B) receptors in transfected BE(2)-C neuroblastoma cells is inhibited by RGS4. J Neurochem. 2000;75(3):934–8.
95. Philp LK, Butler MS, Hickey TE, Butler LM, Tilley WD, Day TK. SGTA: a new player in the molecular co-chaperone game. Horm Cancer. 2013;4(6):343–57.
96. Fliss AE, Benzeno S, Rao J, Caplan AJ. Control of estrogen receptor ligand binding by Hsp90. J Steroid Biochem Mol Biol. 2000;72(5):223–30.
97. Tan Z, Sun X, Hou FS, Oh HW, Hilgenberg LG, Hol EM, et al. Mutant ubiquitin found in Alzheimer's disease causes neuritic beading of mitochondria in association with neuronal degeneration. Cell Death Differ. 2007;14(10):1721–32.
98. van Leeuwen FW, Hol EM, Fischer DF. Frameshift proteins in Alzheimer's disease and in other conformational disorders: time for the ubiquitin-proteasome system. J Alzheimers Dis. 2006;9(3 Suppl):319–25.
99. van Tijn P, de Vrij FM, Schuurman KG, Dantuma NP, Fischer DF, van Leeuwen FW, et al. Dose-dependent inhibition of proteasome activity by a mutant ubiquitin associated with neurodegenerative disease. J Cell Sci. 2007;120(Pt 9):1615–23.
100. Govindarajulu M, Ramesh S, Shankar T, Kora MK, Moore T, Dhanasekaran M. Role of neddylation in neurodegenerative diseases. NeuroSci. 2022;3(4):533–45.
101. Schmidt MF, Gan ZY, Komander D, Dewson G. Ubiquitin signalling in neurodegeneration: mechanisms and therapeutic opportunities. Cell Death Differ. 2021;28(2):570–90.
102. Mori F, Nishie M, Piao YS, Kito K, Kamitani T, Takahashi H, et al. Accumulation of NEDD8 in neuronal and glial inclusions of neurodegenerative disorders. Neuropathol Appl Neurobiol. 2005;31(1):53–61.
103. Dil Kuazi A, Kito K, Abe Y, Shin RW, Kamitani T, Ueda N. NEDD8 protein is involved in ubiquitinated inclusion bodies. J Pathol. 2003;199(2):259–66.
104. Hara Y, Waters EM, McEwen BS, Morrison JH. Estrogen effects on cognitive and synaptic health over the lifecourse. Physiol Rev. 2015;95(3):785–807.
105. Appleman ML, Thomas JL, Weiss AR, Nilaver BI, Cervera-Juanes R, Kohama SG, et al. Effect of hormone replacement therapy on amyloid beta (Abeta) plaque density in the rhesus macaque amygdala. Front Aging Neurosci. 2024;15:1326747.
106. Ahmed T, Zulfiqar A, Arguelles S, Rasekhian M, Nabavi SF, Silva AS, et al. Map kinase signaling as therapeutic target for neurodegeneration. Pharmacol Res. 2020;160:105090.
107. Newton K, Dixit VM. Signaling in innate immunity and inflammation. Cold Spring Harb Perspect Biol. 2012;4(3):a006049.
108. Shih RH, Wang CY, Yang CM. NF-kappaB signaling pathways in neurological inflammation: a mini review. Front Mol Neurosci. 2015;8:77.
109. Du Y, Du Y, Zhang Y, Huang Z, Fu M, Li J, et al. MKP-1 reduces Aβ generation and alleviates cognitive impairments in Alzheimer's disease models. Signal Transduct Target Ther. 2019;4:58.
110. Weber K, Erben RG, Rump A, Adamski J. Gene structure and regulation of the murine epithelial calcium channels ECaC1 and 2. Biochem Biophys Res Commun. 2001;289(5):1287–94.
111. Lee GS, Jeung EB. Uterine TRPV6 expression during the estrous cycle and pregnancy in a mouse model. Am J Physiol Endocrinol Metab. 2007;293(1):E132–8.
112. Kumar S, Singh U, Singh O, Goswami C, Singru PS. Transient receptor potential vanilloid 6 (TRPV6) in the mouse brain: distribution and estrous cycle-related changes in the hypothalamus. Neuroscience. 2017;6(344):204–16.
113. Walters GC, Usachev YM. Mitochondrial calcium cycling in neuronal function and neurodegeneration. Front Cell Dev Biol. 2023;11:1094356.
114. Echeverry S, Rodriguez MJ, Torres YP. Transient receptor potential channels in microglia: roles in physiology and disease. Neurotox Res. 2016;30(3):467–78.
115. Smani T, Gomez LJ, Regodon S, Woodard GE, Siegfried G, Khatib AM, et al. TRP channels in angiogenesis and other endothelial functions. Front Physiol. 2018;9:1731.
116. Cameron VA, Autelitano DJ, Evans JJ, Ellmers LJ, Espiner EA, Nicholls MG, et al. Adrenomedullin expression in rat uterus is correlated with plasma estradiol. Am J Physiol Endocrinol Metab. 2002;282(1):E139–46.
117. Ikeda K, Arao Y, Otsuka H, Kikuchi A, Kayama F. Estrogen and phytoestrogen regulate the mRNA expression of adrenomedullin and adrenomedullin receptor components in the rat uterus. Mol Cell Endocrinol. 2004;223(1–2):27–34.
118. Jerat S, Kaufman S. Effect of pregnancy and steroid hormones on plasma adrenomedullin levels in the rat. Can J Physiol Pharmacol. 1998;76(4):463–6.
119. Watanabe H, Takahashi E, Kobayashi M, Goto M, Krust A, Chambon P, et al. The estrogen-responsive

adrenomedullin and receptor-modifying protein 3 gene identified by DNA microarray analysis are directly regulated by estrogen receptor. J Mol Endocrinol. 2006;36(1):81–9.
120. Serrano J, Uttenthal LO, Martinez A, Fernandez AP, Martinez de Velasco J, Alonso D, et al. Distribution of adrenomedullin-like immunoreactivity in the rat central nervous system by light and electron microscopy. Brain Res. 2000;853(2):245–68.
121. Kato J, Kitamura K, Uemura T, Kuwasako K, Kita T, Kangawa K, et al. Plasma levels of adrenomedullin and atrial and brain natriuretic peptides in the general population: their relations to age and pulse pressure. Hypertens Res. 2002;25(6):887–92.
122. Taylor MM, Samson WK. A possible mechanism for the action of adrenomedullin in brain to stimulate stress hormone secretion. Endocrinology. 2004;145(11):4890–6.
123. Xu Y, Krukoff TL. Adrenomedullin in the rostral ventrolateral medulla increases arterial pressure and heart rate: roles of glutamate and nitric oxide. Am J Physiol Regul Integr Comp Physiol. 2004;287(4):R729–34.
124. Fernandez AP, Masa JS, Guedan MA, Futch HS, Martinez-Murillo R. Adrenomedullin expression in Alzheimer's brain. Curr Alzheimer Res. 2016;13(4):428–38.
125. Ferrero H, Larrayoz IM, Martisova E, Solas M, Howlett DR, Francis PT, et al. Increased levels of brain adrenomedullin in the neuropathology of Alzheimer's disease. Mol Neurobiol. 2018;55(6):5177–83.
126. Macheda ML, Rogers S, Best JD. Molecular and cellular regulation of glucose transporter (GLUT) proteins in cancer. J Cell Physiol. 2005;202(3):654–62.
127. Zhang Y, Chen K, Sloan SA, Bennett ML, Scholze AR, O'Keeffe S, et al. An RNA-sequencing transcriptome and splicing database of glia, neurons, and vascular cells of the cerebral cortex. J Neurosci. 2014;34(36):11929–47.
128. Scott H, Panin VM. N-glycosylation in regulation of the nervous system. Adv Neurobiol. 2014;9:367–94.
129. Scott H, Panin VM. The role of protein N-glycosylation in neural transmission. Glycobiology. 2014;24(5):407–17.
130. Murrey HE, Gama CI, Kalovidouris SA, Luo WI, Driggers EM, Porton B, et al. Protein fucosylation regulates synapsin Ia/Ib expression and neuronal morphology in primary hippocampal neurons. Proc Natl Acad Sci USA. 2006;103(1):21–6.
131. Li X, Nott SL, Huang Y, Hilf R, Bambara RA, Qiu X, et al. Gene expression profiling reveals that the regulation of estrogen-responsive element-independent genes by 17 beta-estradiol-estrogen receptor beta is uncoupled from the induction of phenotypic changes in cell models. J Mol Endocrinol. 2008;40(5):211–29.
132. Chen Z, Yu Q, Yu Q, Johnson J, Shipman R, Zhong X, et al. In-depth site-specific analysis of N-glycoproteome in human cerebrospinal fluid and glycosylation landscape changes in Alzheimer's disease. Mol Cell Proteomics. 2021;20:100081.
133. Guan XM, Yu H, Jiang Q, Van Der Ploeg LH, Liu Q. Distribution of neuromedin U receptor subtype 2 mRNA in the rat brain. Brain Res Gene Expr Patterns. 2001;1(1):1–4.
134. Iwai T, Iinuma Y, Kodani R, Oka J. Neuromedin U inhibits inflammation-mediated memory impairment and neuronal cell-death in rodents. Neurosci Res. 2008;61(1):113–9.
135. Khaksari M, Maghool F, Asadikaram G, Hajializadeh Z. Effects of sex steroid hormones on neuromedin S and neuromedin U2 receptor expression following experimental traumatic brain injury. Iran J Basic Med Sci. 2016;19(10):1080–9.
136. Vigo E, Roa J, Pineda R, Castellano JM, Navarro VM, Aguilar E, et al. Novel role of the anorexigenic peptide neuromedin U in the control of LH secretion and its regulation by gonadal hormones and photoperiod. Am J Physiol Endocrinol Metab. 2007;293(5):E1265–73.
137. DeNardo DG, Kim HT, Hilsenbeck S, Cuba V, Tsimelzon A, Brown PH. Global gene expression analysis of estrogen receptor transcription factor cross talk in breast cancer: identification of estrogen-induced/activator protein-1-dependent genes. Mol Endocrinol. 2005;19(2):362–78.
138. Hu D, Dong X, Wang Q, Liu M, Luo S, Meng Z, et al. PCP4 promotes Alzheimer's disease pathogenesis by affecting amyloid-beta protein precursor processing. J Alzheimers Dis. 2023;94(2):737–50.
139. Penugurti V, Khumukcham SS, Padala C, Dwivedi A, Kamireddy KR, Mukta S, et al. HPIP protooncogene differentially regulates metabolic adaptation and cell fate in breast cancer cells under glucose stress via AMPK and RNF2 dependent pathways. Cancer Lett. 2021;10(518):243–55.
140. Seyfried NT, Dammer EB, Swarup V, Nandakumar D, Duong DM, Yin L, et al. A multi-network approach identifies protein-specific co-expression in asymptomatic and symptomatic Alzheimer's disease. Cell Syst. 2017;4(1):60-72e4.
141. Tandon R, Levey AI, Lah JJ, Seyfried NT, Mitchell CS. Machine learning selection of most predictive brain proteins suggests role of sugar metabolism in Alzheimer's disease. J Alzheimers Dis. 2023;92(2):411–24.
142. Karamese M, Aksak S, Gundogdu OB, Unal B. A new hypothesis about hematopoietic Pbx-interaction protein (HPIP): can it be a key factor in neurodegeneration in the post-menopausal period? Med Hypotheses. 2013;81(3):470–6.
143. Yang J, AlTahan A, Jones DT, Buffa FM, Bridges E, Interiano RB, et al. Estrogen receptor-alpha directly regulates the hypoxia-inducible factor 1 pathway associated with antiestrogen response in breast cancer. Proc Natl Acad Sci USA. 2015;112(49):15172–7.
144. Xu X, Yang M, Zhang B, Dong J, Zhuang Y, Ge Q, et al. HIF-1alpha participates in secondary brain injury through regulating neuroinflammation. Transl Neurosci. 2023;14(1):20220272.
145. Shou Y, Koroleva E, Spencer CM, Shein SA, Korchagina AA, Yusoof KA, et al. Redefining the role of lymphotoxin beta receptor in the maintenance of lymphoid organs and immune cell homeostasis in adulthood. Front Immunol. 2021;12:712632.
146. Osorio J. Reproductive endocrinology: less estrogen, more neuroinflammation? Nat Rev Endocrinol. 2012;8(7):381.
147. Dejardin E, Droin NM, Delhase M, Haas E, Cao Y, Makris C, et al. The lymphotoxin-beta receptor induces different patterns of gene expression via two NF-kappaB pathways. Immunity. 2002;17(4):525–35.
148. Li F, Oh I, Kumar S, Eteleeb A, Gupta A, Buchser W, et al. Loss of estrogen unleashing neuro-inflammation increases

the risk of Alzheimer's disease in women. bioRxiv. 2022. https://doi.org/10.1101/2022.09.19.508592.
149. Walker DG. Defining activation states of microglia in human brain tissue: an unresolved issue for Alzheimer's disease. Neuroimmunol Neuroinflammation. 2020;7:194–214.
150. Wu WF, Tan XJ, Dai YB, Krishnan V, Warner M, Gustafsson JA. Targeting estrogen receptor beta in microglia and T cells to treat experimental autoimmune encephalomyelitis. Proc Natl Acad Sci USA. 2013;110(9):3543–8.